

THE PRODUCTION AND MEASUREMENT OF AN ULTRASONIC FIELD

12  
7/2

A THESIS

Presented to

the Faculty of the Division of Graduate Studies

Georgia School of Technology

In Partial Fulfillment

of the Requirements for the Degree

Master of Science in Physics

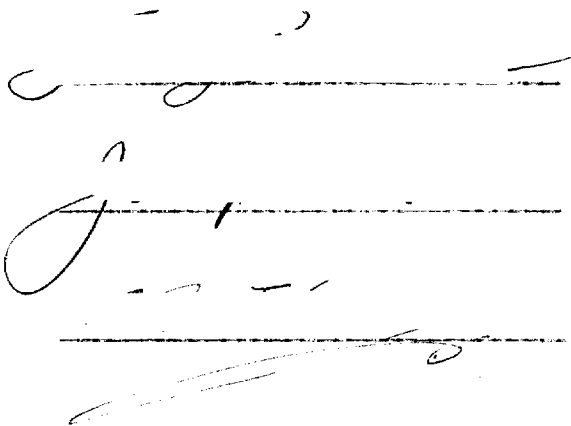
by

David Maxwell Barton

June 1947

## The Production and Measurement of an Ultrasonic Field

Approved:

Three handwritten signatures are written on three horizontal lines. The first signature is a cursive 'C' followed by a horizontal stroke. The second signature is a large cursive 'J' followed by a horizontal stroke. The third signature is a cursive 'S' followed by a horizontal stroke. To the right of the second signature is a small handwritten 'd'.Date Approved by Chairman June 3, 1947

## ACKNOWLEDGEMENTS

I should like to express my great appreciation to Dr. F. E. Lowance of the Physics Department for his advice, interest and time so generously given to this thesis problem. I should also like to thank J. Q. Williams of the Physics Department, S. C. Bailey, and T. W. Kethley of the State Engineering Experiment Station.

This work was done under contract to the Tennessee Valley Authority, Georgia School of Technology Project 98.

## TABLE OF CONTENTS

CHAPTER	PAGE
ACKNOWLEDGEMENTS . . . . .	iii
I. DEFINITION OF THE PROBLEM AND DESCRIPTION OF PRINCIPLES INVOLVED . . . . .	1
II. DESCRIPTION OF APPARATUS AND CONSIDERATIONS INCORPORATED IN THE DESIGN . . . . .	17
III. MEASUREMENT OF THE ABSOLUTE SOUND INTENSITY BY RADIATION PRESSURE MEASUREMENT	
MEASUREMENT BY SPHERES . . . . .	33
MEASUREMENT BY AIR VANE . . . . .	37
MEASUREMENT BY COPPER SULPHATE PROBE . . . . .	44
IV. PROPERTIES OF THE SOUND FIELD AND MISCELLANEOUS GRAPHS . .	53
SUMMARY. . . . .	60
BIBLIOGRAPHY AND REFERENCES . . . . .	78
APPENDICES	
I. THEORY OF FOX METHOD FOR MEASURING ABSOLUTE SOUND INTENSITY. . . . .	61
METHODS . . . . .	62
RESULTS . . . . .	64
CONCLUSIONS . . . . .	64
II. THEORY OF FOX, HERTZFELD AND ROCK METHOD FOR MEASURING ABSOLUTE SOUND INTENSITY . . . . .	66
III. PROCEDURE USED IN OBTAINING AN ACCURATE FREQUENCY RESPONSE CURVE FOR THE TRANSDUCER . . . . .	69
IV. ESTIMATION OF MAXIMUM RELATIVE ERROR . . . . .	71



## LIST OF TABLES

	PAGE
Table I Physical Properties of the Two Spheres . . . . .	72
Table II Data on the Measurement of the Cross-Section of the Field . . . . .	73
Table III Data for Calibration of Voltage Amplifier and Power Amplifier. . . . .	74
Table IV Calibration Data for Voltage Input Vs. Sonic Output for the Ammonium Phosphate Crystal Transducer . . . . .	75
Table V Voltage Calibration Data for the High Sensitivity Inverse Feedback Voltage Amplifier . . . . .	76
Table VI Frequency Response Data for the Driver and Transducer . . . . .	77

## LIST OF FIGURES

	PAGE
Figure 1 Sketch of a Quartz Plate . . . . .	4
Figure 2 Modes of Vibration of Quartz Plates . . . . .	7
Figure 3 Electrical Equivalent of a Crystal . . . . .	8
Figure 4 An Ultrasonic Black Box . . . . .	13
Figure 5 Block Diagram of Elements in $\text{CuSO}_4$ Sound Detector . .	18
Figure 6 The $\text{CuSO}_4$ Probe . . . . .	19
Figure 7a Circuit Diagram of the Driver Unit . . . . .	21
Figure 7b Blueprint of the Transducer . . . . .	22
Figure 8 Testing Tank . . . . .	26
Figure 9 Reflector Plate . . . . .	29
Figure 10 Support Stand. . . . .	30
Figure 11 Track for Support and Reflector . . . . .	31
Figure 12 Circuit Diagram of the Inverse Feedback Amplifier . .	32
Figure 13 Forces on a Sphere in a Liquid Medium Containing a Progressive Sound Wave . . . . .	35
Figure 14 Sketch of an Air Vane . . . . .	39
Figure 15 Components Used in the Air Vane Radiation Pressure Measurement . . . . .	40
Figure 16 Calibration Curve for Two Glass Fibers . . . . .	41
Figure 17 A Typical Cross-Section of the Sound Beam . . . . .	43
Figure 19 Block Diagram of Components for Calibration of Inverse Feedback Amplifier. . . . .	46
Figure 20 Calibration Curves for the Inverse Feedback Amplifier.	48
Figure 21 Calibration Curves for the Inverse Feedback Amplifier.	49

# THE PRODUCTION AND MEASUREMENT OF AN ULTRASONIC FIELD

## SECTION I

### DEFINITION OF THE PROBLEM AND DESCRIPTION OF PRINCIPLES INVOLVED

The problem which concerns this thesis is the production and measurement of an ultrasonic field in a liquid medium.

There are two physical properties of matter that prove to be of use in generating high frequency sound waves in a liquid medium.

The first is the magnetostriction property which is a change in the physical dimensions of a ferromagnetic material when brought into the presence of a magnetic field. The change in dimension is independent of the sign of the field and may be an increase or decrease, depending on its magnetization and the temperature. This effect will disappear above the Curie point of the material. The only two ferromagnetic substances that show a regular variation in dimensions, with no inversions, are nickel and annealed cobalt. The fractional change in length of a rod of nickel and cobalt at saturation is of the order  $10^{-6}$ . By causing a rod to vibrate at its fundamental frequency, it is possible to increase this factor to  $10^{-4}$ . The natural periods of a vibrating rod are given by the expression,

$$f = \frac{k}{2l} \sqrt{\frac{E}{\rho}} \quad (1)$$

$k = 1, 2, 3,$   
 $E = \text{elastic constant}$   
 $\rho = \text{density}$   
 $l = \text{length of the rod}$

For maximum output it is desirable to work at the fundamental frequency. Examination of the above equation and consideration of physical dimensions for nickel or cobalt lead to an upper frequency limit of about 100,000 c.p.s. (for fractional lengths of the order of 3 cm.). As a rule these generators are rather temperamental and will not exhibit frequency stability under different load conditions at the high end of the frequency limit. For certain limited uses, however, in the frequency range 10,000 to 50,000 c.p.s., they are superior to any other means of generating sound fields. The effect was discovered by Joule<sup>1</sup> about 1846.

In order to produce fields from the range 300,000 c.p.s. to 30,000,000 c.p.s., it is necessary to utilize the second property, the piezoelectric effect discovered by J. and P. Curie<sup>2</sup> circa 1880. Some crystals such as quartz, rochelle salt, tourmaline, and cane sugar will develop charges across certain crystal planes, when subjected to tension or compression. The size of the charge depends on the substance and the orientation of the surface with respect to the axis of the mother crystal. The charge reverses when the tension is changed to compression. The requirement for a crystal to exhibit this phenomenon is that it have one or more polar axes or lack a center of symmetry. A polar axis is defined as an imagined direction in the crystal, the two ends of which are not equivalent. This means that the crystal cannot be interchanged to give the original physical shape by rotating the crystal through 180° about an axis at right angles to the polar axis.

The three crystals most frequently used are quartz, rochelle salt and ammonium phosphate. The latter, a recent product produced by the Brush Development Company in Cleveland, has a higher piezo constant than

either rochelle salt or quartz, and is sufficiently strong mechanically to compare with quartz. The most widely used generator of very high frequency and high intensity sound is quartz. Quartz crystals for this purpose are superior to rochelle salt crystal whose main disadvantage lies in the fact that they lose their piezo property above 120° F. At room temperature the piezo constant for rochelle is about 1000 times that of quartz and for work in which the operating temperature is kept low, rochelle salt may be used. It is not as rugged a material as quartz.

If a piezo crystal cut in the proper fashion is placed in an alternating electric field, then the inverse Curie effect is observed so that the size of the crystal changes and thus produces tension and compression as the sign of the electric field varies.

Referring to Figure 1 we note the following:

1. Positive charge on the surface b-l and negative charge on the opposite face produce expansion in the X direction.
2. Positive charge on the surface l-b and negative charge on the opposite face likewise produce expansion of the faces d-b in the y direction.

Reversal of sign causes change from expansion to contraction and vice versa.

The amount of expansion or contraction in the X-longitudinal direction is represented by  $S_x$ , and is proportional to the applied potential difference between the faces,

$$S_x = d_{11} V \quad (2)$$

and likewise for the y direction (transverse),

SKETCH OF A TYPICAL  
CRYSTAL BLANK

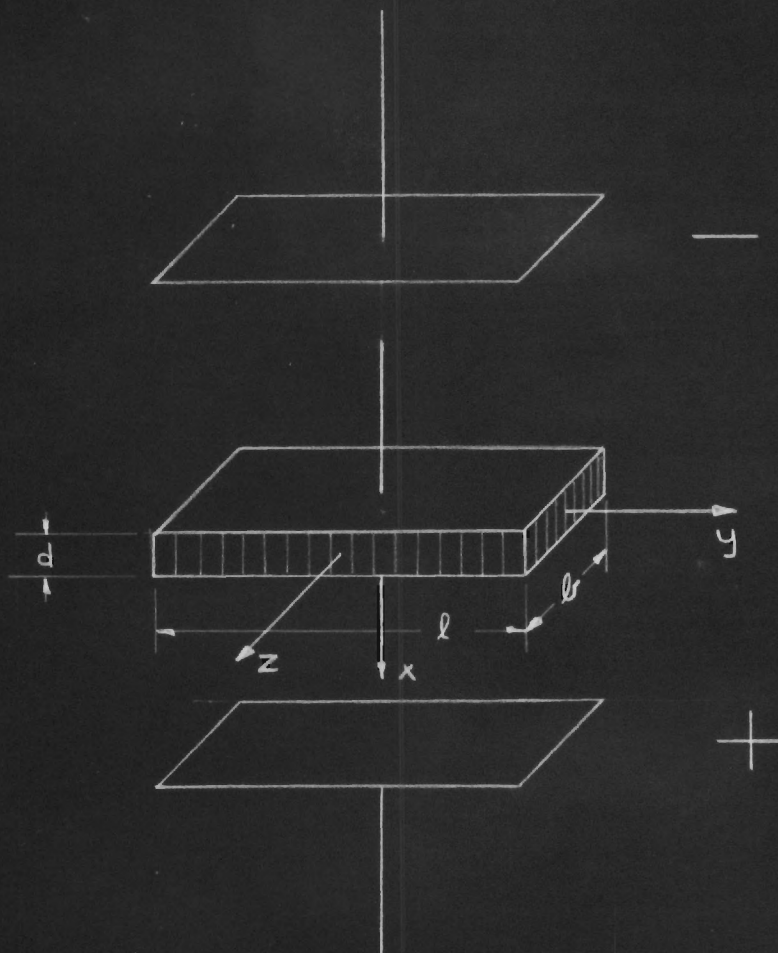


Figure 1

$$S_y = d_{12} V \quad d = \text{piezo modulus} \quad (3)$$

For quartz,  $d_{11} = d_{12} = -6.36 \times 10^{-8} \text{ cm gm sec.}$ , thus for the X direction a potential difference of 3000 volts produces a change of  $6.36 \times 10^{-7} \text{ cm.}$

If an alternating field is now applied between the plates, due to the two reciprocal piezo effects mentioned above two modes of vibration are possible:

1. There can be a thickness vibration in the X direction.
2. Independent of this, a longitudinal vibration of length is observed.

Assuming no coupling between these two vibrations (an infinite plate), the natural period of vibration of a plate may be calculated by using the following relation:

$$N = \frac{1}{2d} \sqrt{\frac{c_{11}}{\rho}} \quad \begin{array}{l} d = \text{thickness of plate (cm)} \\ \rho = \text{density (gm/cm}^3\text{)} \\ c_{11} = \text{a constant for a type} \\ \quad \text{of crystal and mode of} \\ \quad \text{vibration} \end{array} \quad (4)$$

and for quartz plates,

$$\text{density } (\rho) = 2.65 \text{ gm/cm}^3$$

$$c_{11} = 85.46 \times 10^{10} \frac{\text{dyne}}{\text{cm}^2}$$

From these a useful relation follows. N (natural frequency of a quartz plate) equals  $\frac{285,500}{d} \text{ c.p.s.}$

The upper limit for the fundamental of quartz plates is about 50 megacycles, and for tourmaline 150 megacycles. At these frequencies, the plates become very thin, are quite fragile, and are broken by excessive

voltages. Actual coupling between these two modes of vibration causes a slight deviation from the value calculated above and can be used to produce a shearing motion of the plates. By using such crystals it is possible to produce shear waves of high frequency in metals and other elastic solids. (See Figure 2.)

The sharpness at which this natural vibration occurs is very marked and corresponds to an electrical analogy of a resonant circuit with a high  $Q$ . The logarithmic damping is of the order of  $10^{-4}$ . The equivalent circuit is given in Figure 3.

In electrical work the larger the  $Q$  factor of a circuit the more narrow the frequency band at which resonance occurs. As some crystals have values of  $Q$  greater than 500,000 this provides a very narrow band filter. This property is very useful, but in making a source of sound it is desirable to reduce this naturally high  $Q$  by a suitable means of damping. A common way is to plate the crystal with a metal film and then it is possible for the frequency of the driving voltage to vary without losing the large amplitude vibrations of the quartz in its resonance frequency.

In order to make band pass filters it is sometimes possible to combine many resonant circuits whose resonant frequencies are slightly staggered, thus obtaining a "band" pass network which allows a band of frequencies to pass and rejects everything else. This same trick may be used in designing a transducer to produce sound energy from electrical energy, and thus by combining a group of crystals whose resonances are staggered over a given range, a transducer might be produced to operate over an appreciable band of frequencies. Further, by using banks of



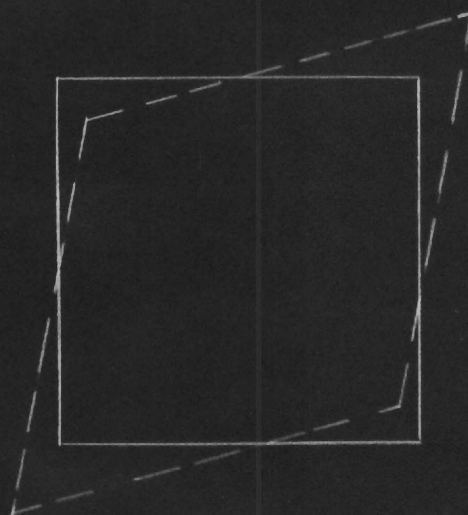
19 7

# MODES OF VIBRATION OF DIFFERENT CUTS OF QUARTZ CRYSTALS



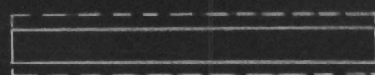
SIDE VIEW

AT CUT



TOP VIEW

CT CUT

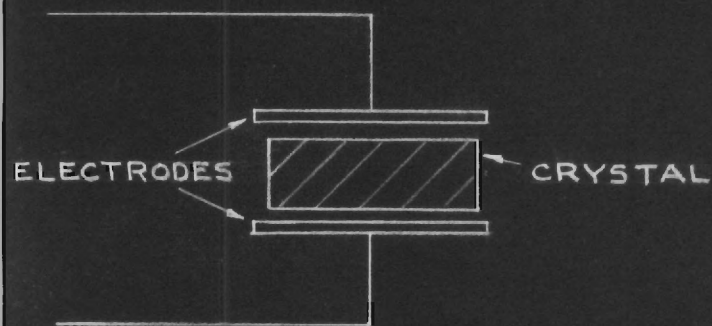


SIDE VIEW

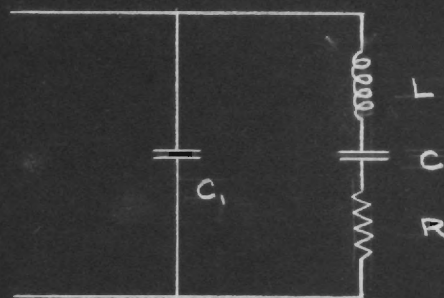
X CUT

Figure 2

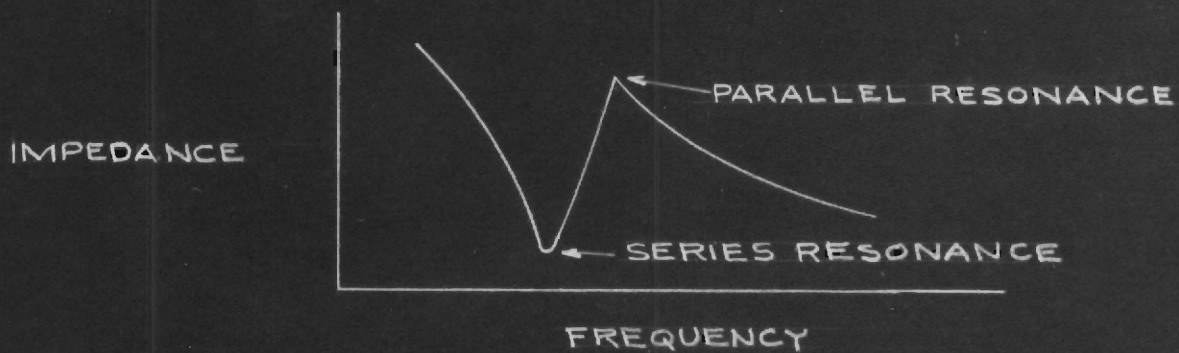
# ELECTRICAL EQUIVALENT OF A VIBRATING CRYSTAL



ACTUAL ARRANGEMENT  
OF CRYSTAL



ELECTRICAL EQUIVALENT



crystals, a source of plane waves may be approximated very closely, producing a well columned beam of sound energy. These two features are utilized in the ammonium phosphate transducer used in the experimental setup.

In the consideration of principles related to measurement of absolute intensity of the sound energy, the following commonly used terms and their symbols are given:

$I$  = the sound intensity and is the amount of sound energy

passing through a unit surface in a unit of time. Some

common units are  $\frac{\text{ergs}}{\text{cm}^2 \text{ s}}$ ,  $\frac{\text{watts}}{\text{cm}^2}$ ,  $\frac{\text{watts}}{\text{in}^2}$ .

$\rho$  = density of the medium through which the sound is conducted.

$v$  = velocity of the sound wave.

$\omega = 2\pi f$   $f$  = frequency of the wave.

$A$  = maximum amplitude of the vibrating particles

$P$  = amplitude of the oscillating sound pressure

$U$  = acoustic quickness (Schallschnelle) or velocity amplitude of the particles.

Some important relations between these quantities are given in the following discussion relative to plane waves.

$$I = \frac{\rho v}{2} (\omega A)^2 \quad (5)$$

The product  $\rho v$  occurs in such a manner as to correspond to impedance in electrical theory, and hence is referred to as "acoustical impedance."

The product  $\omega A$  has the dimensions of velocity and is referred to as "velocity amplitude."

In the above, the characteristic property of wave motion is satisfied whereby the energy of the wave is proportional to the square of the amplitude. Also,

$$I = \frac{\rho v}{2} U^2 \quad (6)$$

as  $\omega \rho v = \frac{P}{A}$  the acoustic hardness (Schallharte) (7)

and

$$\frac{P}{U} = \rho v \quad (8)$$

then

$$I = \frac{P^2}{2 \rho v} = \frac{PU}{2} \quad (9)$$

From these relations it would be necessary to measure P, U, or P and U in order to evaluate I. This can be accomplished by using calibrated crystals resonate at the frequency of the sound field, thus a separate crystal must be used for each frequency. As a result, such a technique, while practical for an investigation with a particular frequency, is inconvenient and expensive for general applications. In the ultrasonic range mechanical receivers such as Raleigh discs are not responsive and the only practical instruments were calibrated quartz crystals until a recent arrangement was perfected by Fox, Hertzfelder, and Rock. This method will be described later.

In the ultrasonic range, however, the intensity of the sound waves

can be made sufficiently high to make measurements of radiation pressure. When sound waves "strike" an object, besides a variation in pressure, a unidirectional force is exerted, which is due to the lack of linearity in the form of the wave equation as indicated by the quadratic terms,

$$\nabla^2 \phi = \frac{1}{v^2} \frac{\partial \phi}{\partial t} \quad \begin{array}{l} \phi = \text{velocity potential} \\ v = \text{velocity of the sound} \end{array} \quad (10)$$

According to Lord Raleigh<sup>3</sup> the sound radiation pressure for a gas is given by the following equation:

$$S = \frac{1}{2}(K + 1)\frac{I}{v} \quad \begin{array}{l} S = \text{radiation pressure} \\ K = \text{ratio of specific heats} \\ I = \text{intensity of sound} \\ v = \text{velocity of sound} \end{array} \quad (11)$$

As  $I \propto P^2$  or  $A^2$ ,  $S$  is proportional to the square of the amplitude of the pressure or particular amplitudes and, as shown for quartz, the amplitude is proportional to the applied potential differences between the crystal faces. Therefore  $S$  should vary as the square of the applied potential. This is also true for ammonium phosphate crystals.

If a vane containing a trapped layer of air is suspended in water, there will be almost 100% reflection of sound energy from the air-water interface. If this vane is then subjected to the radiation pressure, the radiation pressure will be equal to two times the energy density of the sound. Since,

$$E = \frac{I}{v} \quad \text{where } v = \text{velocity of sound in the medium} \quad (12)$$

the radiation pressure  $P$  will be related to the intensity  $I$  by the expression,

$$P = 2E = \frac{2I}{v} \quad (13)$$

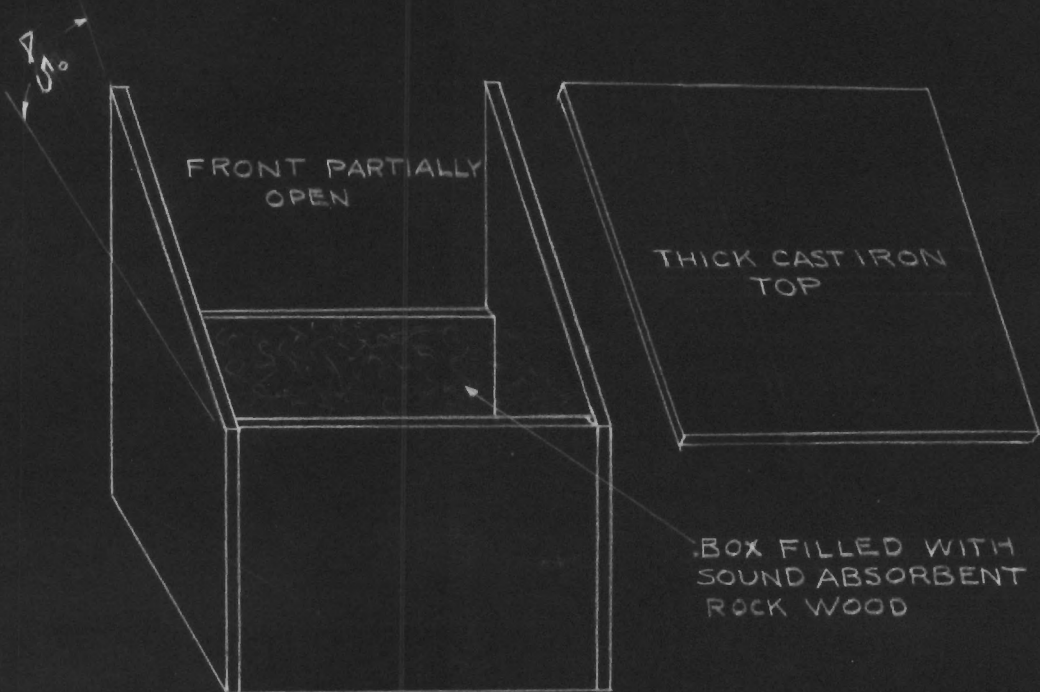
From this relation it is possible to calculate the intensity of the sound from observations of the deflection of an air vane and the constants relating the deflection of the vane to the applied force. The size of the vane is related to the wave length of the sound by considerations of scattering and reflection,<sup>4</sup> and is maximum for approximately  $\frac{D}{\lambda} = 1.2$ , where  $D$  = diameter of the vane and  $\lambda$  = wave length of the sound. For this experiment the vane was 3.1 cm in diameter and the wave length was 2.6 cm. Then,

$$\frac{D}{\lambda} = 1.2$$

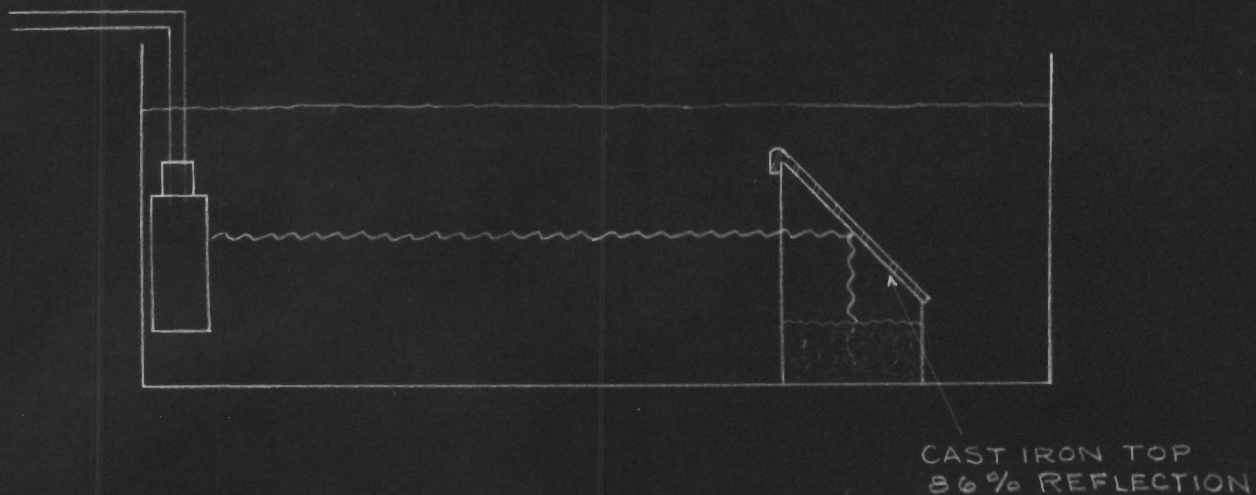
A second method of measurement of the radiation pressure comes from analysis of radiation pressure on a uniform sphere due to a plane wave in an infinite frictionless medium. For this measurement two different sized beads were used. A description of the theory is given in Appendix I. A device shown in Figure 4 for absorbing the sound is provided to simulate the infinite medium, while the transducer is constructed to produce plane waves. Water approximates a frictionless medium for static measurements.

Two relative intensity gauges were constructed by the glass shop but proved insensitive for ultrasonic fields of the magnitude produced by the transducer. These two gauges are suitable only for very intense fields greater than 5 watts/cm<sup>2</sup>. The first gauge was devised by Richards<sup>5</sup>

# SKETCH OF A BLACK BOX FOR ABSORBING SONIC RADIATION



WOODEN BOX



TEST TANK

and consists of a thick walled glass funnel with an exponential opening connected to a capillary. When the funnel and capillary are dipped into the sound field, the radiation pressure forces the water up the capillary and the rise in level is proportional to the intensity.

The second gauge, devised by Greutzmacher<sup>6</sup> conducts the sound by conduction along a solid glass rod to a small bulb filled with air. The air is heated by the sound and, on expansion, operates a gas manometer which reads relative intensities. For the order of magnitude of the field used in these experiments, using a water manometer, no deflection was observed in the one observation made. Further observations were not possible as the gauge was accidentally broken.

Whenever a measurement is made of some quantity, the ideal measuring instrument is the one that causes the least disturbance of the quantity being measured. The radiation measurement devices previously described depend on reflection or absorption of a fair amount of energy incident upon them and so produce varying amounts of deformation of the field in their vicinity. A device described by Rock, Fox, and Hertzfelder<sup>7</sup> appears to produce a small field distortion. The theory of the method is given in Appendix II. This method was used with the following modifications.

1. The frequency range was extended to a minimum of 50 kc.
2. The sensitivity was approximately doubled by using both side bands.

This technique involves the variation of conductivity of a  $\text{CuSO}_4$  solution with the static pressure, the change in conductivity being due to the change in concentration and change in viscosity. For water above 4° F. a rather unusual property exists in the decrease in viscosity for an increase in pressure. Both the viscosity and activity effects are



additive and so exercise a relative increase in conductivity of  $10^{-6}$ .

Analysis of this technique can be made by considering a sound wave of frequency  $f_s$  traveling through a water medium in which a  $\text{CuSO}_4$  solution enclosed in a container is immersed. The acoustical impedance of the container and the water are equal so the sound wave will travel unattenuated through the  $\text{CuSO}_4$  solution. If two fine electrodes are inserted into the  $\text{CuSO}_4$  solution and insulated from the water, the current that flows between the electrodes, through the  $\text{CuSO}_4$ , will be a function of the potential difference between the electrodes, as well as the conductivity of the solution.

If the conductivity of the solution, which is actually an impedance because of polarization effects, is made small compared to the source of current, the small change in resistance will not appreciably affect the current and we have a constant current source. The resistance of the solution will vary as the pressure due to the ultrasonic wave changes, the change in resistance being proportional to the change in pressure. If the resistance at any time is  $R$  and the resistance of the solution at normal pressure is  $R_0$ , then

$$R = R_0 (1 - Sp \cos 2\pi f_s t) \quad (14)$$

where  $S$  is the relative increase in conductance per atmosphere and  $p$  is the pressure applied to the solution in atmospheres.

If the constant current generator provides a current at a frequency  $f_1$  and with constant amplitude, then the current through the solution with no sound will be,

$$I = \frac{\sqrt{2} E_{\text{eff}} \cos 2\pi f_1 t}{R_o} \quad \text{where } E_{\text{eff}} = \text{R.M.S. voltage at electrodes} \quad (15)$$

If the sound of frequency  $f_s$  passes through the solution then there will be a small alternating voltage appearing across the electrodes.

$$E = I R = \frac{\sqrt{2} E_{\text{eff}} \cos 2\pi f_1 t}{R_o} \frac{R_o}{1 - Sp \cos 2\pi f_s t} \quad (16)$$

On expansion, assuming a non-linear mixing,

$$E = \sqrt{2} E_{\text{eff}} \left\{ \cos 2\pi f_1 t + \frac{1}{2} Sp \cos 2\pi (f_1 + f_s) + \frac{1}{2} Sp \cos 2\pi (f_1 - f_s) \right\} \quad (17)$$

Thus two side bands, frequency  $f_1 - f_s$  and  $f_1 + f_s$  have appeared, the voltage associated with each frequency being  $1/2 E_{\text{eff}} Sp$ . For a  $\text{CuSO}_4$  solution, we would then expect a signal with each side band of 115 microvolts per applied volt at the electrodes per atmosphere pressure. (See Appendix II.)

## SECTION II

## DESCRIPTION OF APPARATUS AND CONSIDERATIONS INCORPORATED IN DESIGN

A schematic diagram is given in Figure 5 of the elements involved in the sound generator and the  $\text{CuSO}_4$  detector. Their functions are as follows:

1. A resistance-capacity oscillator was designed to operate at approximately 50 to 250 kc with an output of 15 volts.
2. The 15 volts output is fed into a 6L6 voltage amplifier which produces a signal of some 100 volts at  $1/2$  watt and thus furnishes the following power amplifier with a large signal.
3. The 807 power amplifier is operated class C, biased about 50 volts below cut-off with 700 volts on the plate. The output is about 300 volts at 50 kc which is fed into the transducer.
4. The ammonium phosphate crystal transducer is immersed in the water and produces a sound field which is a function of the applied voltage, the frequency of the electromagnetic driving energy, the geometry of the boundaries of the field, the temperature of the water, the density of the water, the nature of the bounding surfaces, and other less important related factors. This sound energy is transferred through the water to the detecting device.

For the  $\text{CuSO}_4$  detector the elements involved are:

1. The probe, shown in Figure 6, contains the  $\text{CuSO}_4$  and the two Pt electrodes. The conductivity changes at the rate of the incident sound and thus modulates the low frequency constant current.
2. The modulated signal is fed into a high sensitivity, constant

BLOCK DIAGRAM OF COMPONENTS  
USED WITH  $\text{CuSO}_4$  DETECTOR

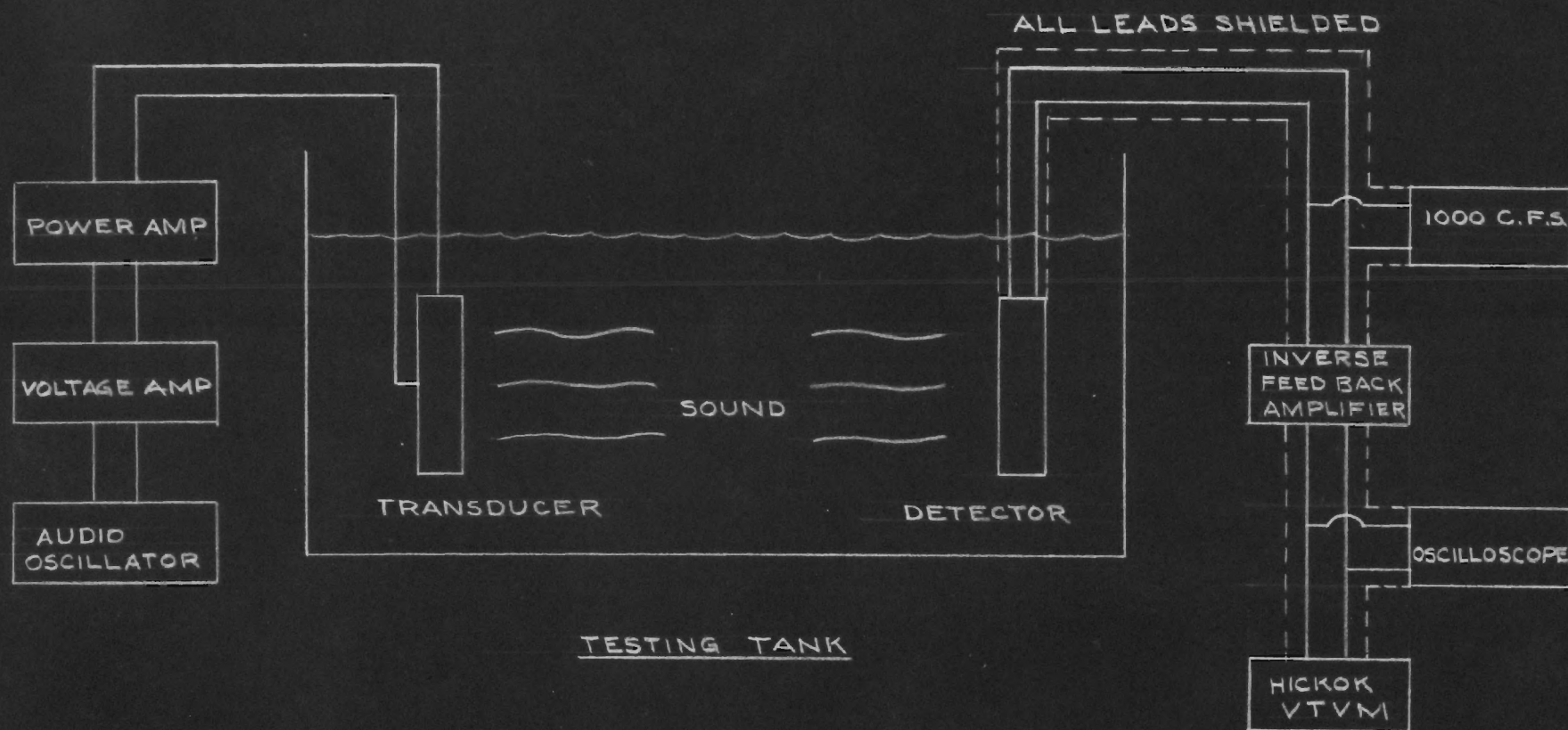
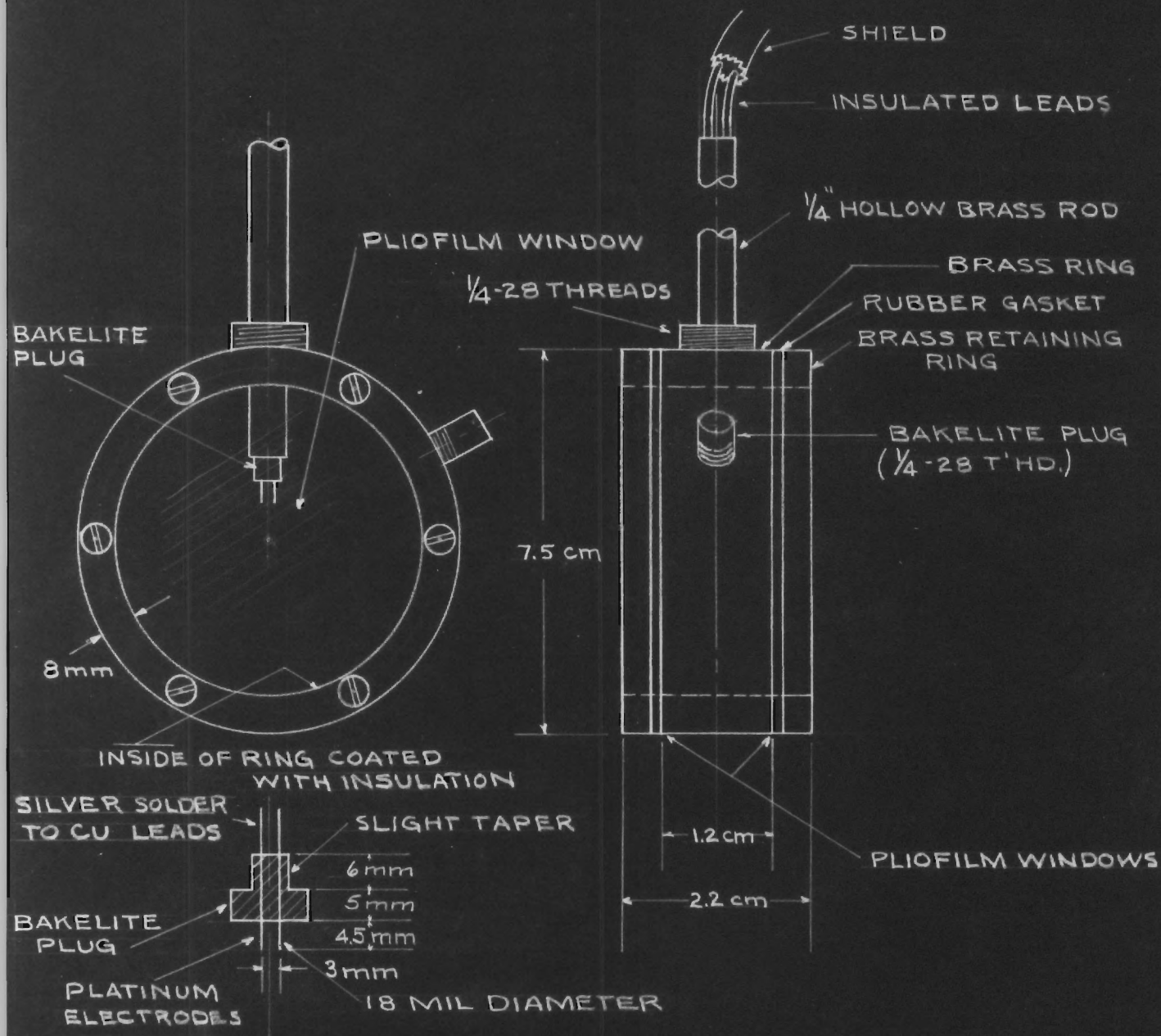


Figure 5

# CuSO<sub>4</sub> PROBE FOR INVESTIGATING SOUND FIELDS



gain band pass amplifier which selects the 50 kc modulation and amplifies it.

3. A Hewlett-Packard audio oscillator or a Clough-Brengle, is used as a source of constant current.

4. The amplified signal is detected and the output read on a Hickok vacuum tube voltmeter. In order to study the wave shape of the amplified signal, a Dumont cathode ray oscilloscope is connected to the cathode of the cathode follower in the high-gain voltage amplifier.

The various radiation pressure gauges are placed at the center of the beam of sound energy about 40 cm from the transducer.

A more complete description of each of these elements is given in the following text.

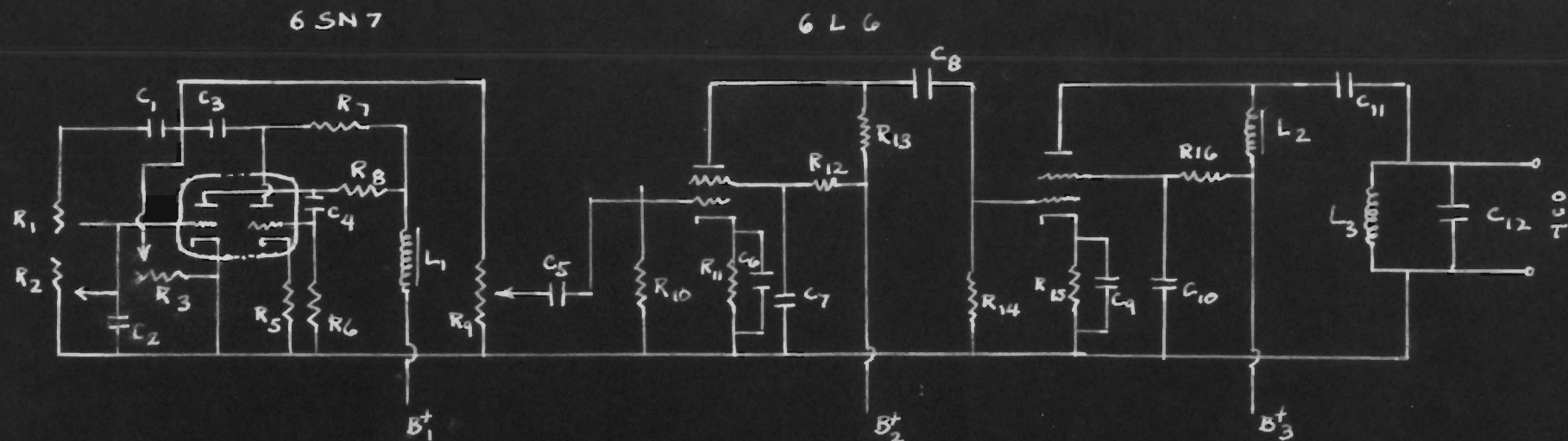
The R-C Oscillator. A common oscillator for low frequency work is the R-C type oscillator that was used in this experiment.<sup>8</sup> Such oscillators provide good frequency stability and a wide tuning range as well as avoiding the use of inductances which would be physically large in size for this frequency range. The circuit diagram for the oscillator is given in Figure 7.

The condition for stable oscillation is when the voltage across grid to ground of input is equal to the output voltage across  $C_1 R_1$ , so then,

$$f = \frac{1}{2\pi \sqrt{R_1 R_2 C_1 C_2}} \quad (f = \text{resonate frequency})$$

and if

$$R_1 = R_2 \text{ and } C_1 = C_2$$



$C_1 \& C_2 = 4-50 \text{ MMFD}$   
 $C_3 = .01 \text{ MFD}$   
 $C_4 = .05 \text{ "}$   
 $C_5 = .25 \text{ "}$   
 $C_6 = .1 \text{ "}$   
 $C_7 = .1 \text{ "}$   
 $C_8 = .1 \text{ "}$   
 $C_9 = .1 \text{ "}$   
 $C_{10} = .1 \text{ "}$   
 $C_{11} = .1 \text{ "}$   
 $C_{12} = .0001 \text{ MFD}$

$R_1 \& R_2 \& R_3 = 100,000 \text{ OHM (POT)}$   
 $R_5 = 1,500 \text{ " 1WATT}$   
 $R_6 = 500,000 \text{ " "}$   
 $R_7 \& R_8 = 50,000 \text{ " "}$   
 $R_9 = 25,000 \text{ " (POT)}$   
 $R_{10} = 470,000 \text{ " 1/2 WATT}$   
 $R_{11} = 220 \text{ " 5 "}$   
 $R_{12} = 24,000 \text{ " 1 "}$   
 $R_{13} = 8500 \text{ " 2 "}$   
 $R_{14} = 330,000 \text{ " 1/2 "}$   
 $R_{15} = 400 \text{ " 5 "}$   
 $R_{16} = 100,000 \text{ " 1 "}$

$L_1 = 2.5 \text{ MH CHOKE}$   
 $L_2 = 70 \text{ MH CHOKE}$   
 $L_3 = 600 \text{ MH.}$   
 TANK INDUCTANCE

$B_1^+ \& B_2^+ = 250 \text{ V}$   
 $B_3^+ = 700 \text{ V}$

719 Figure 7

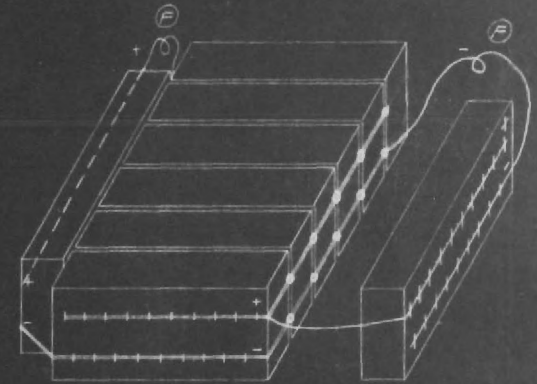
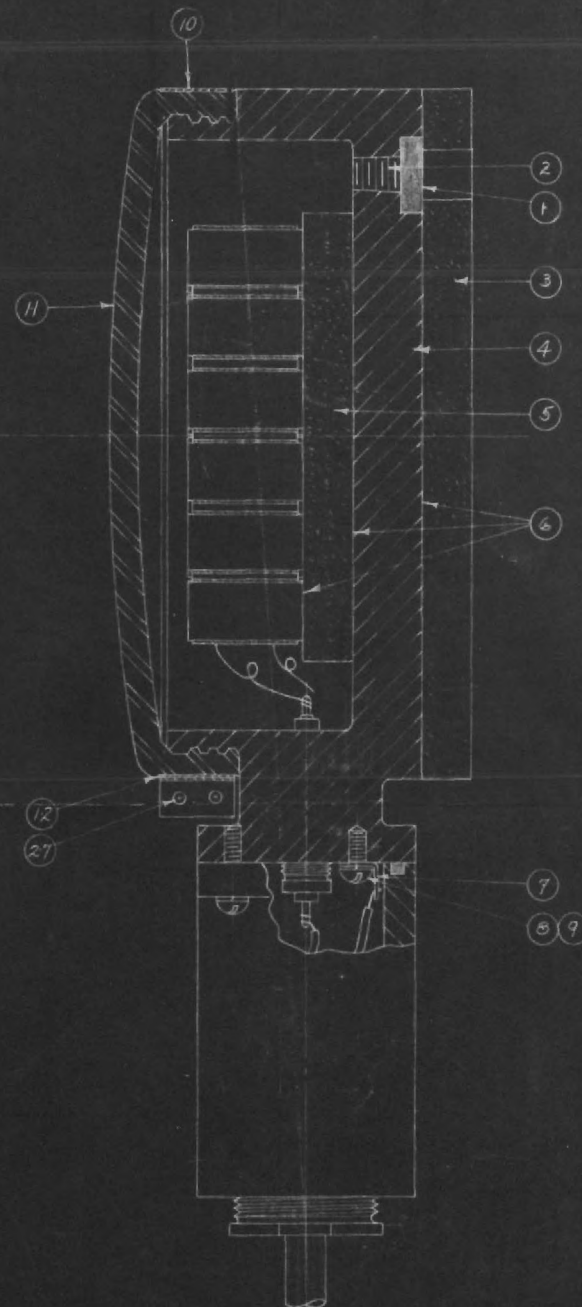
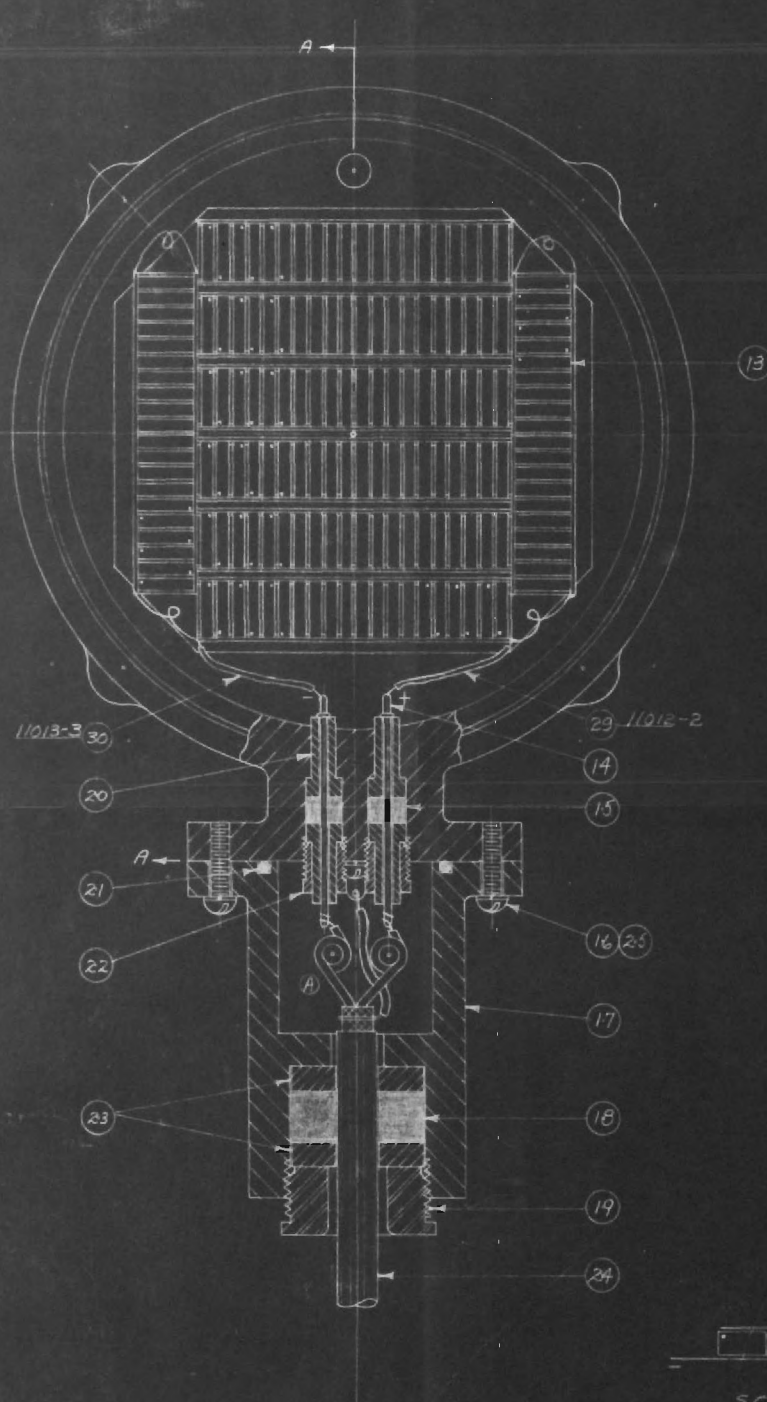


No. 400,167

SERIAL

Used on

Model AX-173-1

PERSPECTIVE SHOWING  
LEAD CONNECTIONS

## CHANGED

A	DETAIL 1-4-46	216
B	NOTE REVISED	216
C	U.S. 200726-303	216
D	CO # 3963	216
E	ITEMS 25430 CORRECTION	216
F	ALTERNATE	216
G	ITEMS 25430 CORRECTION	216
H	BY CUSTOMER 225-4 W.T.D.	216

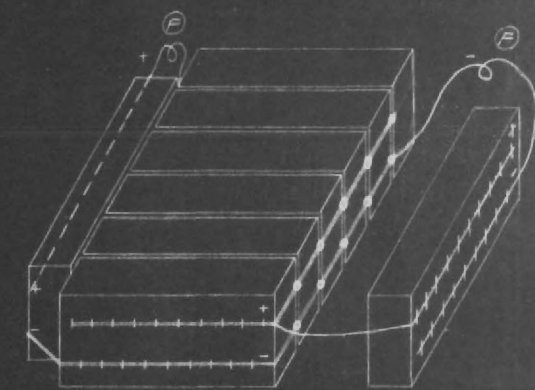
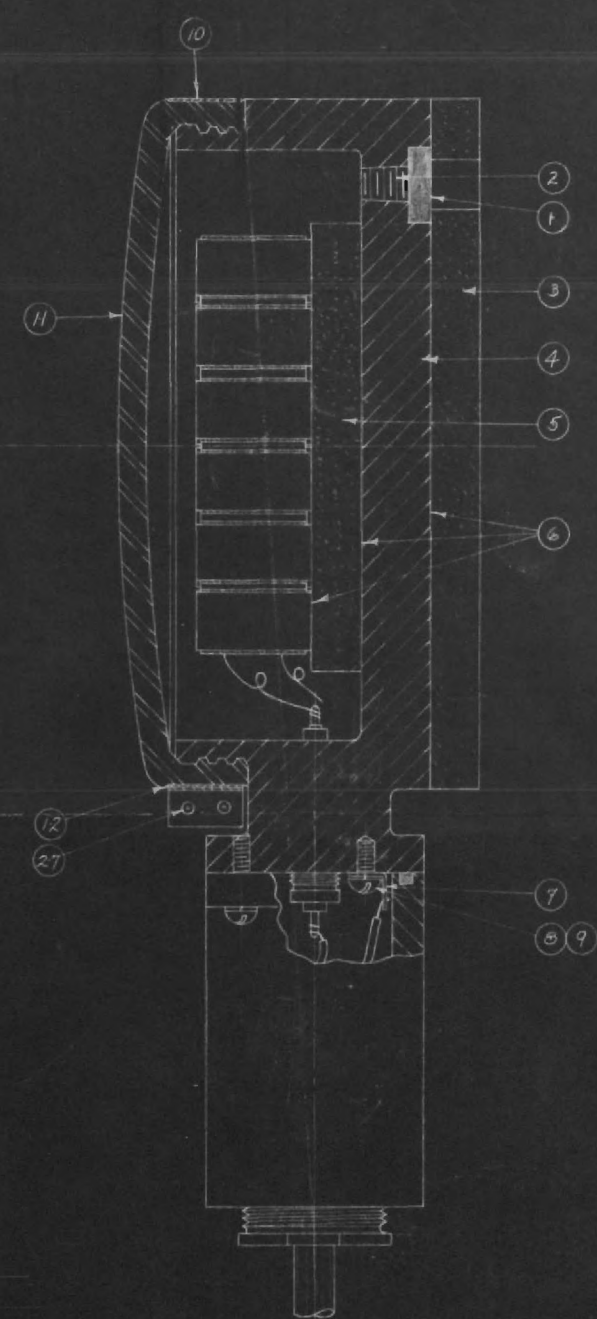
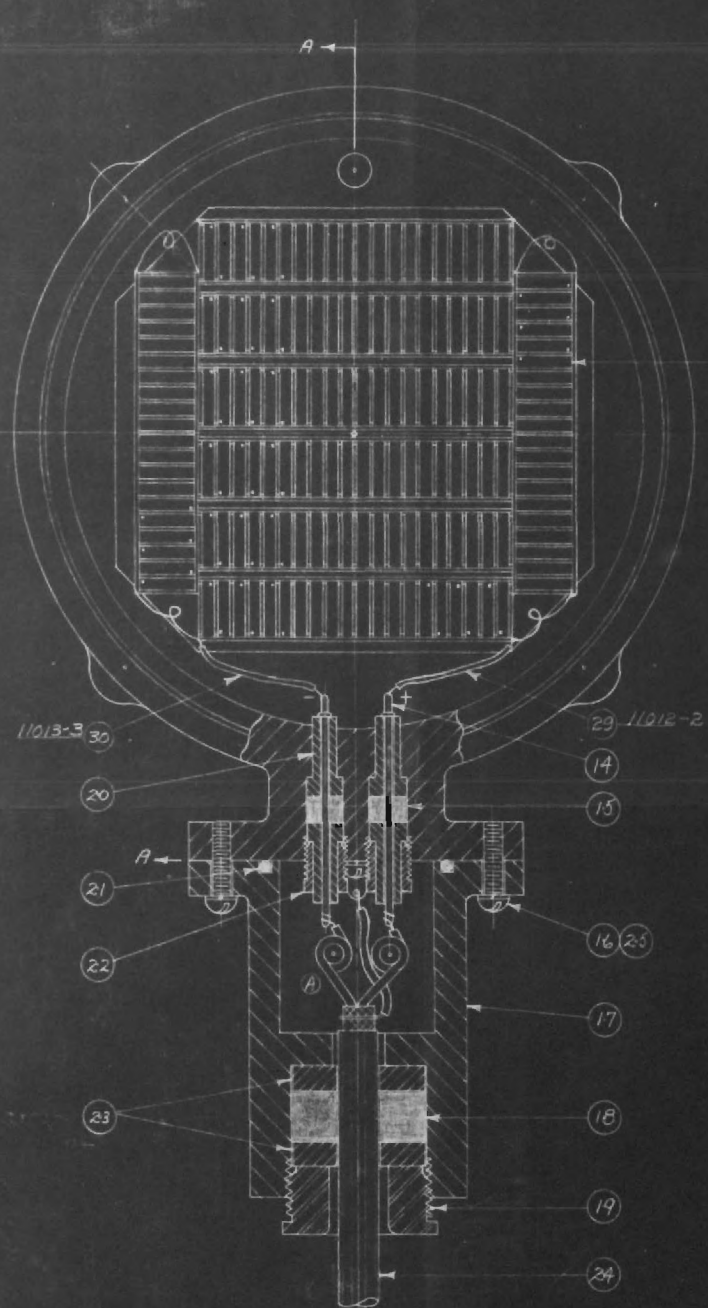
B EVACUATE APPROXIMATELY 30 MINUTES AFTER  
REACHING A VACUUM OF 125 MICRONS AND  
INJECT OIL UNDER SUFFICIENT  
PRESSURE TO BULGE CAP  $\frac{1}{4}$  TO  $\frac{3}{8}$

NOTE: COAT ALL EXPOSED CORPENE PER P.S. 5097

Issued OCT 25 1946

Date 12-18-45 Scale 1-1





PERSPECTIVE SHOWING  
LEAD CONNECTIONS



SCHEMATIC

⑧ EVACUATE APPROXIMATELY 30 MINUTES AFTER  
REACHING A VACUUM OF 125 MICRONS AND  
INJECT OIL UNDER SUFFICIENT  
PRESSURE TO BULGE CAP  $\frac{1}{2}$  TO  $\frac{3}{8}$

NOTE: COAT ALL EXPOSED CORPENE PER P.S. 5097

CHANGED		
A	DETAIL 1-4-46	WJS
B	NOTE REVISED	WJS
C	WIRE 220726-503	WJS
D	CO # 963	WJS
E	1-9-46 WJS	WJS
F	DRUMS CO # 503	WJS
G	ADDED 1-9-46 WJS	WJS
H	ITEM TO BE PROVIDED BY CUSTOMER 2-23-46 WJS	WJS

Issued OCT 25 1946
Date 12-13-45 Scale 1-1
Drawn W.J.D. Check WJS
Appr. Eng. WJS
Appr. Prod.

RF - Rough Finish  
F - Smooth Tool Finish (Std)  
FF - Polished Finish

Allowable Tolerance  $\pm .001$  Unless Otherwise Specified

and we assume a value of 100,000 ohms for  $R_1$  then (a) C must be as given below for a frequency of 40 kc.

$$4 \times 10^4 = \frac{1}{2\pi} 10^5 C_1^{-1} \quad C_1 = C_2 = 40 \times 10^{-12} \text{fds}$$

(b) For the high frequency end, let  $f = 200$  kc,

$$\frac{200}{40} = \frac{40}{X} X = C_1 = 8 \times 10^{-12} \text{fds}$$

and  $C_1 = C_2 = 8$  to 40 microfarads.

The minimum additional capacitance of  $C_1$ , which is in parallel with the input capacitance of the tube, will be only 4.6 microfarads. This input capacity is the limiting factor in the high frequency response of an R-C oscillator.

A feedback arrangement to limit the oscillator and preserve the wave shape is provided by resistance  $R_3$ .

With this design, the oscillator covers a range from 30 to 250 kc and has an output of some 15 volts. In order to get a sine wave from the oscillator it is necessary to synchronize both variable resistances and both capacitances. It is found that the amount of feedback will change the frequency so it is necessary to include this in the calibration of the frequency response.

The 6L6 Voltage Amplifier. The stage following the 6SN7 is the 6L6 which is capacitively coupled to its output. This stage is operated class A with a cathode bias, with 250 volts on the plate and is capacitively coupled to the following 807 power stage.

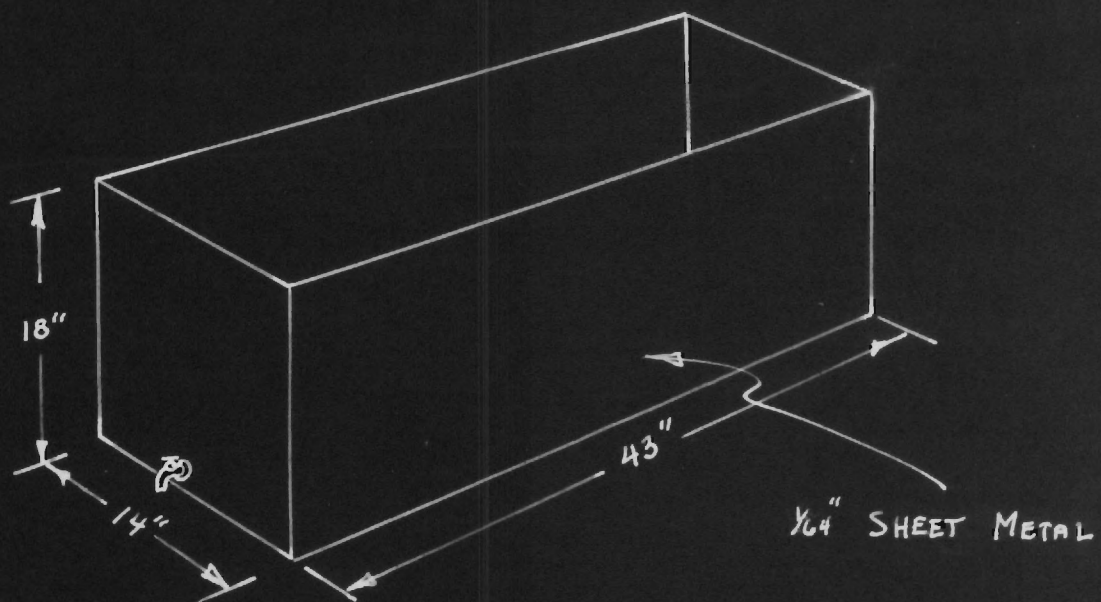
The 807 Power Amplifier. The 807 power amplifier tube is rated at

45 watts output with 700 volts on the plate. It is operated at about one half its rated output and is biased at -45 volts below its cut-off voltage and is driven by a grid signal from the voltage amplifier of 60 to 80 volts. The bias is obtained by a cathode resistor and the screen is also dropped to 300 volts from the plate voltage by means of a resistor. The stage is capacitively coupled to the tank coil which consists of an inductance of 700 microhenries in parallel with the inductance and capacity of the transducer and a fixed capacitance of .0001 microfarads. The maximum R.F. output at 50 kc is 500 volts with no load and 300 volts with the load.

The Ammonium Phosphate Crystal Transducer. A description of the mechanical construction of the transducer is given in the blueprint of Figure 7b. There are 160 crystals arranged in eight banks of twenty each. These crystals are all connected in parallel and are placed end on so as to radiate from the small end face of the rectangular parallelepiped crystal blanks. This gives a plane wave of fine directional properties, and the resonate frequencies of the crystals are supposed to be such that there will be a band width of 30 to 70 kc although this was not observed. There is a primary resonance at 57 kc and several other minor resonances. The sensitivity of the detecting devices are such that the sonic output at other than these resonances is not indicated. One of the faces of the crystal is completely insulated from the case and the other face is essentially at ground potential. All of the crystals are immersed in an atmosphere of silicon oil which acts as an insulator and also conducts the sound to the diaphragm that separates the oil from the water. The acoustical impedances of the oil, the diaphragm and the water are all matched to give maximum energy transfer to the water. This transducer then

is designed for use in a water medium and, as a result of this fact, no other medium has been used in this study. The  $\text{CuSO}_4$  detector is also designed for use only in a water medium. The whole crystal assembly is water tight and may be completely submerged. In order to reduce the radiation in the backward direction and therefore increase the amount of energy radiated in the forward direction, the crystals are mounted on a backing of fairly low density. The oil medium may be changed by removing a plug from the rear of the assembly, and other oils inserted, depending upon the use that is to be made of the transducer.

Testing Tank and Accessories. The size of the testing tank was limited by the space available. Consequently, it is rather small and does not provide enough space to set up a proper system for absorbing sound radiation and studying the propagation characteristics of the beam over any appreciable distance. The tank shown in Figure 8 is made of sheet metal and mounted in a wooden box for support. It is about four feet long, two feet wide and two and one half feet high. There is a track mounted on the bottom of the tank on which the transducer mount may slide. (See Figures 9, 10, 11.) At the other end of the track is a reflecting plate provided for the investigation of standing wave patterns. For the investigation of traveling waves there is provided a black box whose function is the absorption of as much of the incident sound energy as possible. This box was constructed with a heavy iron top inclined at an angle of 45 degrees, so as to reflect the sound wave into the box. Fourteen per cent of the sound energy is absorbed at the iron surface, and the remainder is almost completely absorbed by the rock wool in the box. There is also a frame of screen made to place along the sides which is filled with rock wool and thus minimizes the reflections from the



THE TANK IS MOUNTED IN A WOODEN BOX

TRANSDUCER TEST TANK

Figure 8

walls. This arrangement simulates a wave in an infinite medium.

High-Gain, Inverse Feedback, Voltage Amplifier. When the low frequency (1 kc) electromagnetic constant current is modulated by the high frequency sound wave, there is then produced by this action two additional frequencies referred to as side bands. These side bands would occur at 51 and 49 kc if a 1 kc signal were used which would then be modulated at 115 microvolts for each of the side bands per applied volt and atmosphere. As the pressure amplitude of the sound would be of the order of one fifth atmosphere, and assuming that the input would be of the order of one half volt at 1 kc, 10 microvolts could be expected from each side band. By amplifying both side bands the signal would then be 20 microvolts, which is sufficient, if the noise level could be kept down to about 4 microvolts. A band pass arrangement was incorporated to suppress the 1 kc signal and by shielding the amplifier it would be theoretically possible to eliminate the 50 kc electromagnetic radiation from the power amplifier. An inverse feedback was provided so that an out-of-phase signal from the output was fed back into the input and there would be constant amplification of both large and small signals. This feedback also provides a way of controlling the gain and exercises some control over the amplifier, preventing oscillations arising from feedback between stages. A convenient way of measuring the output of the amplifier is to rectify the signal from the cathode of a cathode follower. A single tube can be used for the cathode follower and for the detector if the 6SN7 is used. The grid and plate of one of the triodes is connected together to make a detector, and if this is connected to a DC vacuum tube voltmeter, the rectified AC output appears as a DC reading on the vacuum tube voltmeter. In order to

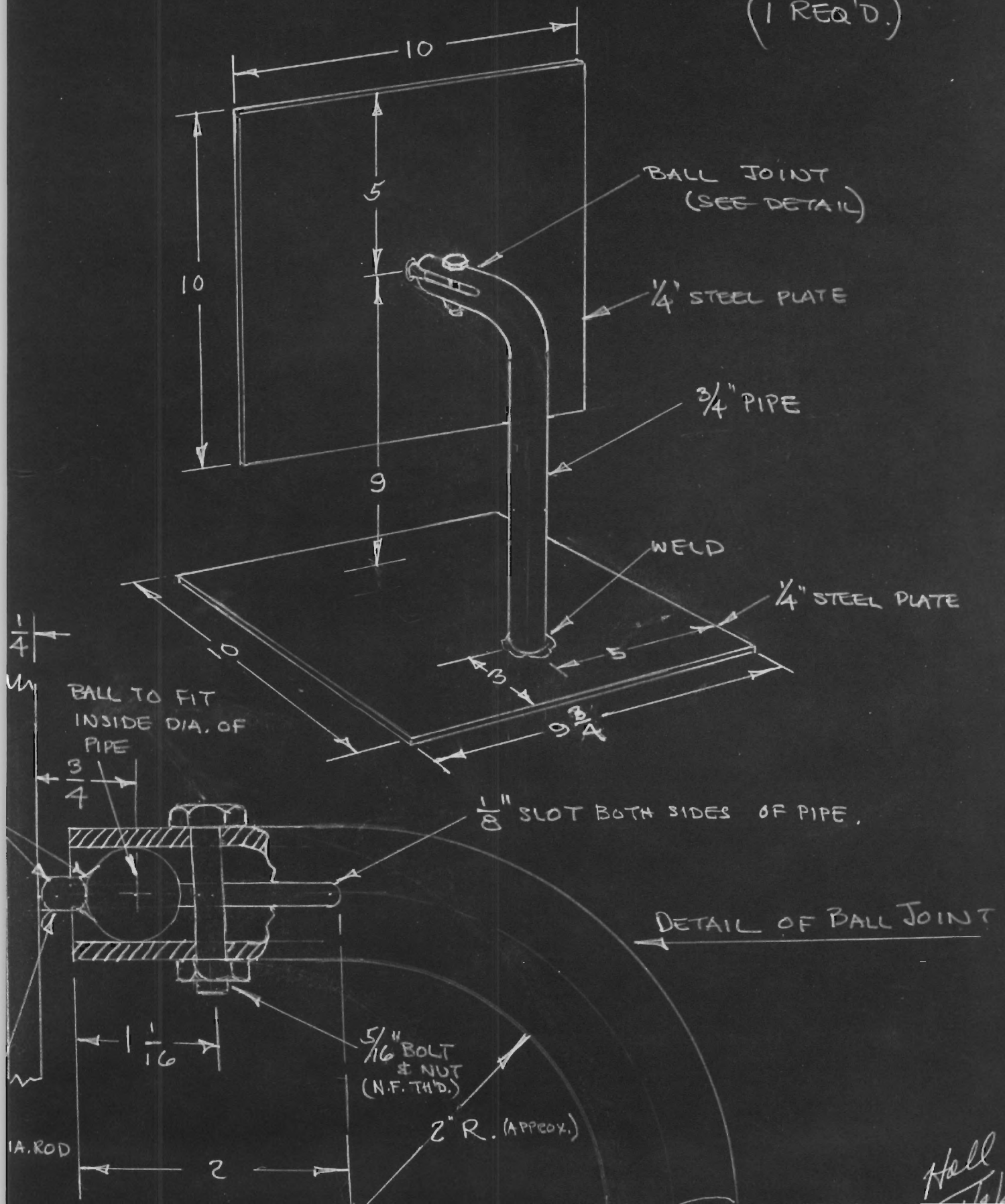
see the wave shape of the output of the amplifier an additional connection was made to the top of the cathode of the cathode follower so that a Dumont oscilloscope could be connected to the circuit. Care was taken to filter out the 60 cycle frequency. All plates, filaments and screens were by-passed with large capacities and a large electrolytic condenser was placed across the B plus. A regulated power supply was used. The amplifier was carefully shielded by isolating the first two stages, shielding the input and output leads, and completely enclosing all stages in a sheet metal chassis. The chassis is used as a common ground, and each stage is grounded to the chassis and to each other. All leads in the first two stages are made as short as conveniently possible.

The overall gain is about 120 db, and the lower half power point is at 30 kc, and the upper half power point is above 70 kc. A circuit diagram is given in Figure 12.

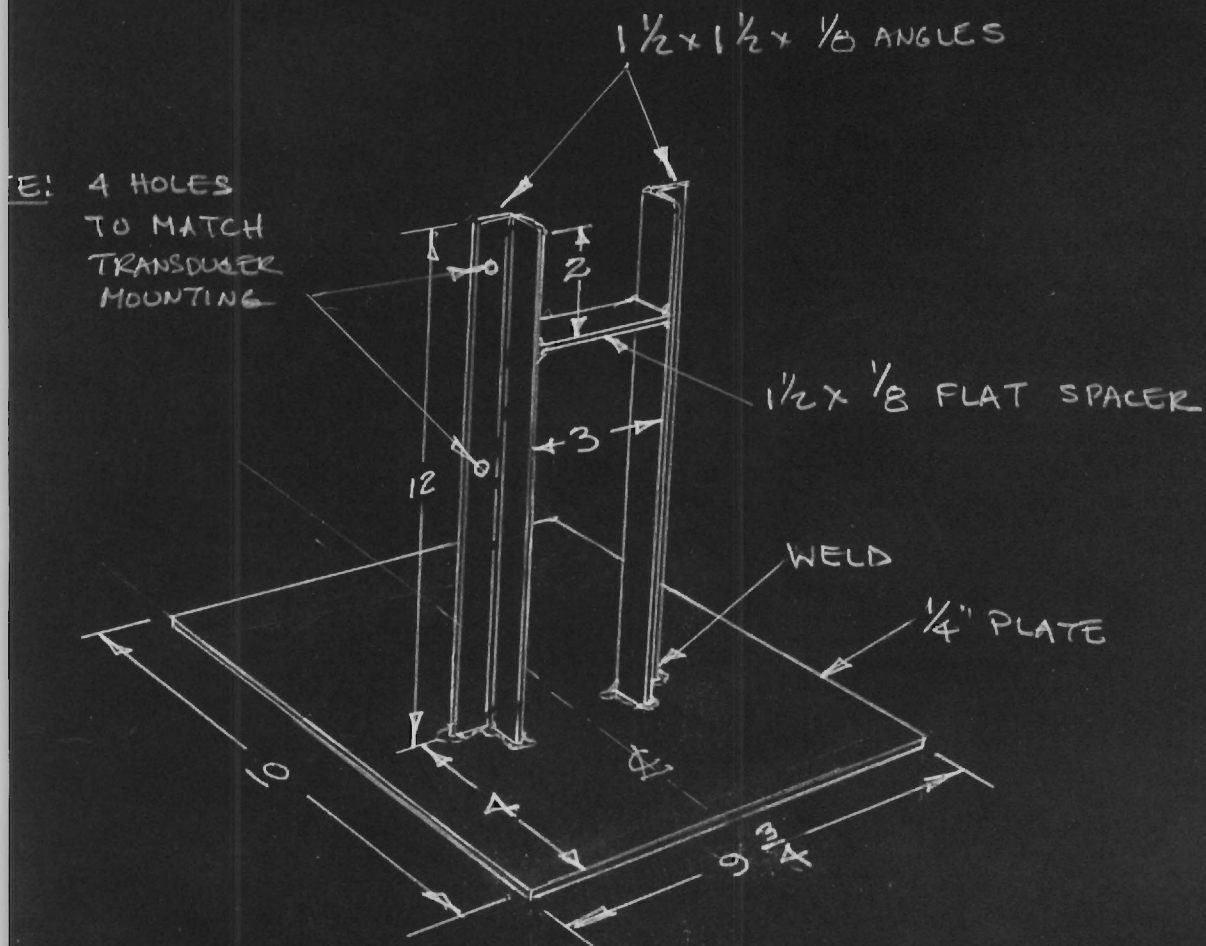


# REFLECTOR PLATE FOR TRANSDUCER TEST TANK

(1 REQ'D.)

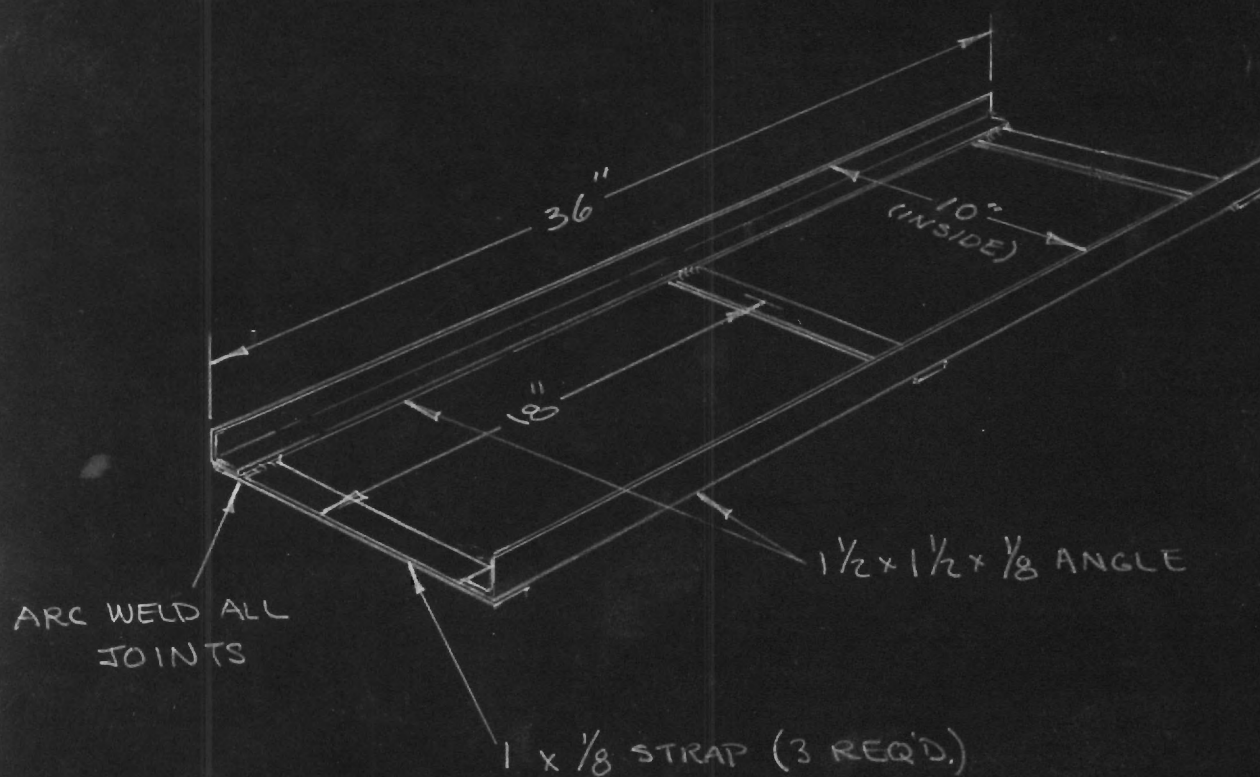






TRANSDUCER SUPPORT STAND - (1 REQ'D.)

Hell  
T. 1/16



FRAME FOR TRANSDUCER TEST TANK  
(1 REQ'D)



## SECTION III

MEASUREMENT OF THE ABSOLUTE SOUND INTENSITY  
BY RADIATION PRESSURE MEASUREMENTSMeasurement by Spheres

Referring to Appendix I, in order to compute the energy density it is necessary to measure the following parameters:

- $\bar{P}$  = the average radiation pressure  
 $\alpha = \frac{2\pi \bar{R}}{\lambda}$        $\bar{R}$  = average radius of the sphere  
 $\lambda$  = wave length of sound in the medium  
 $\rho_o$  = the density of the medium = 1 gm/cm<sup>3</sup>  
 $\rho_s$  = the density of the sphere

The relation of these parameters to the average energy density is as follows:

$F(\rho)$  = a function of the ratio of density of the medium to the density of the sphere.

$$\bar{P} = \rho_o |A|^2 F(\rho) \quad (18)$$

$\bar{P}$  = average radiation pressure.

$\rho_o$  = density of the medium.

$|A|^2$  = the coefficient associated with the velocity potential of the field.

as

$$\bar{E} = \frac{\rho_o k^2 |A|^2}{2} \quad (19)$$

$$k = \frac{2\pi}{\lambda} = \frac{\alpha}{\bar{R}}$$

then we may write  $|A|^2$  in terms of  $\bar{E}$  and substitute in the above,

$$\bar{P} = 2\bar{E} \frac{F(\xi)}{k^2} \quad (20)$$

This expression then evaluates the proportion of the scattered to the reflected energy. As we are evaluating  $E$  by measuring  $P$ , the last equation may be rewritten,

$$\bar{E} = \frac{k^2}{2F(\xi)} \bar{P} \quad (21)$$

Referring to the diagram of Figure 13,  $P$  can be computed by measuring the angle  $\theta$ , and the volume and density of the sphere.

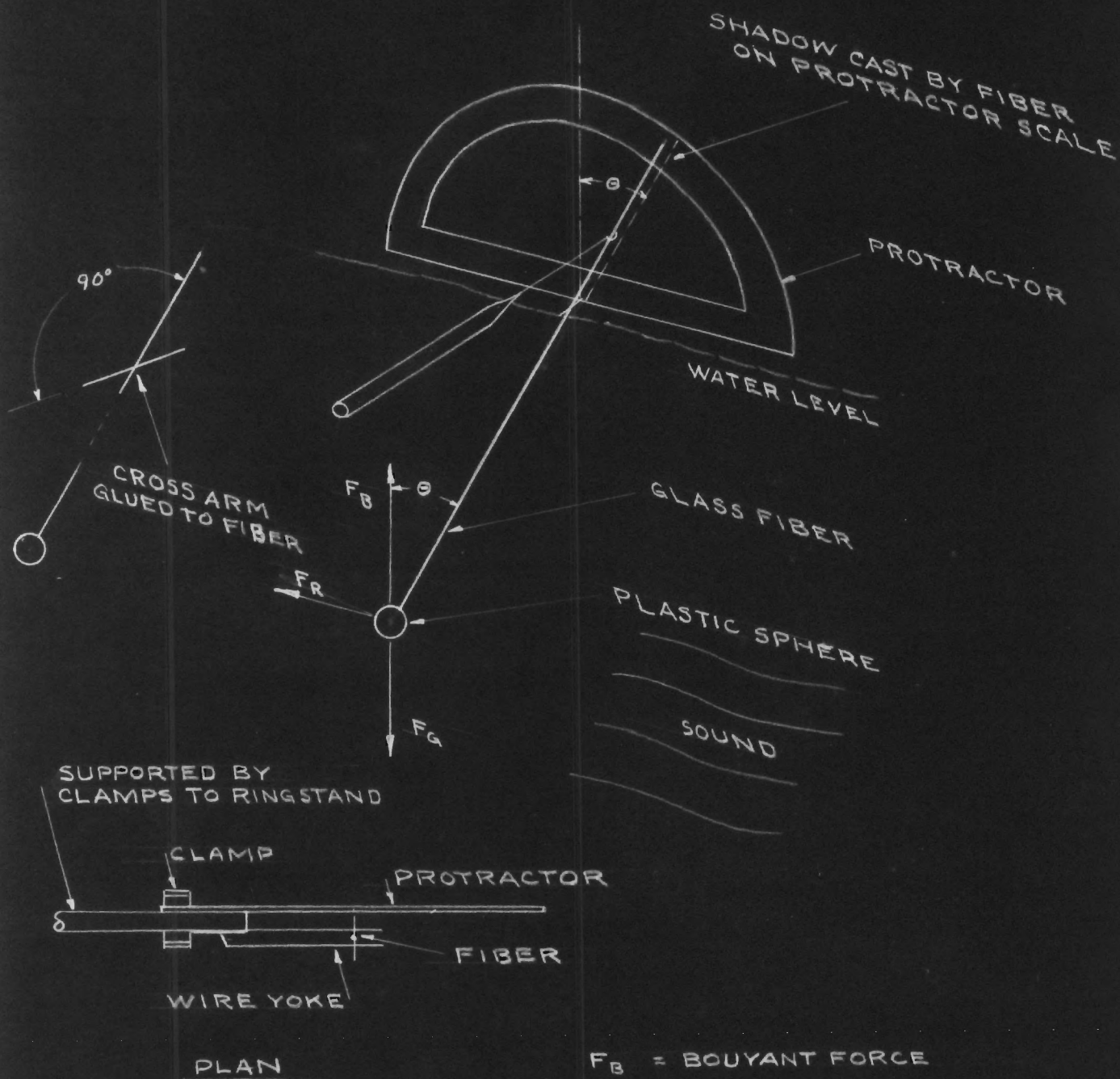
$$F_R = \pi \tilde{\Lambda}^2 \times \bar{P} = (F_G - F_B) \tan \theta \quad (22)$$

$$P = \frac{(F_G - F_B) \tan \theta}{2F(\xi) \pi \tilde{\Lambda}^2} \quad (23)$$

Two spheres were used to compare the effects of using different diameters. Table I lists the measurements of the physical properties of these two spheres and the angle  $\theta$  through which both spheres were deflected by a given sound field. In order to compare the results of the intensity measurements by use of the spheres and by use of the air vane, the air vane was mounted in such a manner as to permit its being placed in the same position relative to the transducer as the spheres. During these measurements the setting of the driving unit for the transducer was not disturbed and the equipment was operated for about two hours to insure complete stability of all components before readings were taken. The frequency of the control oscillator was set at 59 kc and the input to the transducer at 215 volts.



# FORCES ACTING ON A SPHERE SUSPENDED IN A LIQUID MEDIUM CONTAINING A PROGRESSIVE SOUND WAVE



- $F_B$  = BOUYANT FORCE  
 $F_G$  = GRAVITATIONAL FORCE  
 $F_R$  =  $\pi r^2 \times$  RADIATION PRESSURE

Figure 13

When quartz and other crystals are used for generating ultrasonics there is often noticed especially at the higher intensities, an effect referred to as "quartz winds." This is a unidirectional current of air or liquid set in motion by the action of the plates at the crystal-medium surface. On expansion, the medium is pushed forward, but on the subsequent contraction the medium does not collapse quickly enough to follow the plate back and a pumping action results. This current will disturb measurements of radiation pressure so two tests were made to detect its presence.

In the first test a hypodermic needle was filled with black ink and injected into the medium some 3 cm above the position to be investigated for quartz winds. As the ink slowly settled it would expand in a symmetrical pattern such that the diameter of the colored region was about 4 cm by the time it reached the region to be examined. From observations of the behavior of this cloud a current approximately 3 cm in diameter was detected that carried the ink along at .5 cm per second. This current was well columniated and occupied the center of the sound beam. At the edges a much slower current was observed, due partially to the presence of the main stream and to a small extent to the action of the crystals.

When a pliofilm sheet approximately 1/2 mm thick was placed between the transducer and the region of the sound field to be investigated, there was no motion of the medium as indicated by the ink blot test.

In the second test the time required for the vane and the sphere to settle back to its rest position was compared with the sound field on and with it off. These two times agreed sufficiently well to indicate the absence of a moving stream of water.

It may be correctly assumed, therefore, that the deflections observed are due entirely to the radiation pressure.

Taking the values listed in Table I, and finding the correct value for  $F(\xi)$  from Appendix I, substitution in the last equation yields the following value for the energy density:

$$\bar{E} = \frac{k^2 (F_G - F_B) \tan \Theta}{2F(\xi) \pi \bar{h}^2} \quad (24)$$

For Sphere #1,

$$\bar{E}_1 = \frac{(7.80)(.71)(.013)(980)}{2(4.91)(3.14)(.66)} = 3.45 \frac{\text{ergs}}{\text{cm}^3}$$

For Sphere #2,

$$\bar{E}_2 = \frac{7.80(.03)(.026)980}{2(.232)(3.14)(.085)} = 45.0 \frac{\text{ergs}}{\text{cm}^3}$$

The value of  $F(\xi)$  for the small sphere was evaluated by using the expansion in terms of the Bessel function given in Appendix I, equation 1a.

#### Measurement by the Air Vane

The vane could be suspended from the same yoke as the spheres and as its rest position was at the same depth as that of the spheres, it was then possible to remove the spheres and insert the vane into the same field without disturbing any of the apparatus.

In the following procedure for measuring the field at a point by



means of the vane reference is made to Figures 14 and 15.

When the vane was placed in the field, it was deflected 14 degrees or so from its rest position. The calibrated drawn glass fiber was now pressed against a point mid-way between the pivot and the top of the counterpoise of the wire support of the vane, and thus the vane was forced back to its rest position where it is then normal to the field. There is a light source of parallel rays arranged so that the tip of the fiber casts a sharp shadow on the millimeter scale. Its stressed position is recorded and the vane swung back from the zero position so that the fiber can now assume its unstressed position. This reading is recorded and the difference of these two is the deflection of the fiber. From the calibration curve of Figure 16 showing deflection versus deflecting force, the force can be computed and as both lever arms are known, the radiation force can be found. The radiation pressure follows from this, assuming one hundred per cent reflection at the vane.

$$\bar{P} = 2\bar{E}$$

Relating the parameters to the above we have,

$$\bar{E} = \frac{\bar{P}}{2} = \frac{F_R}{2 \pi \lambda^2} \quad (25)$$

but

$$\begin{aligned} F_R \times L_R &= F_F \times L_F \\ F_R &= \frac{L_F}{L_R} F_F = .278 F_F \end{aligned} \quad (26)$$

# SKETCH OF A PENDULUM TYPE VANE FOR RELATIVE AND ABSOLUTE SOUND INTENSITY MEASUREMENTS

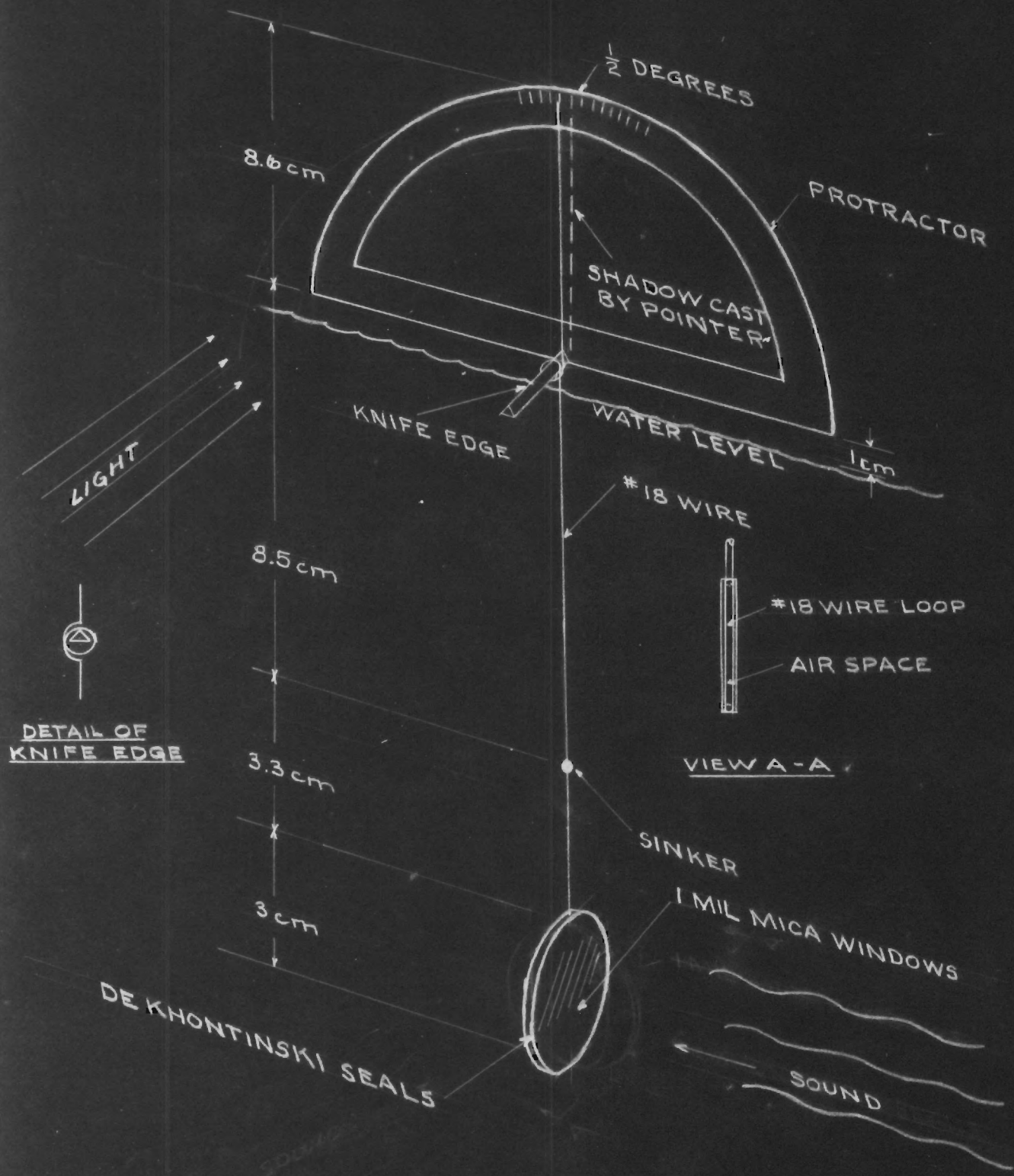


Figure 14

# A DIAGRAM SHOWING COMPONENTS USED IN THE AIR VANE RADIATION PRESSURE MEASUREMENT

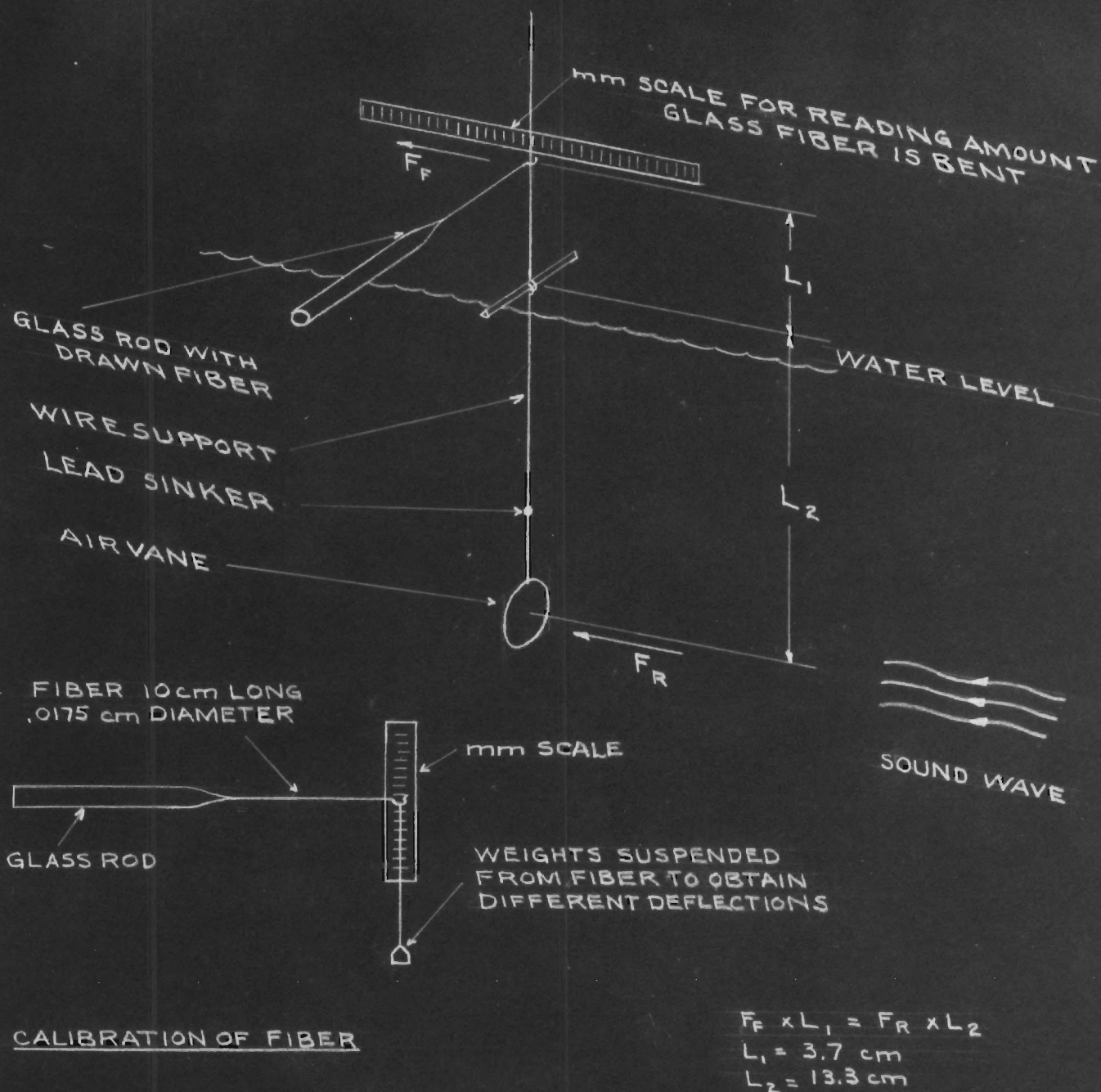


Figure 15

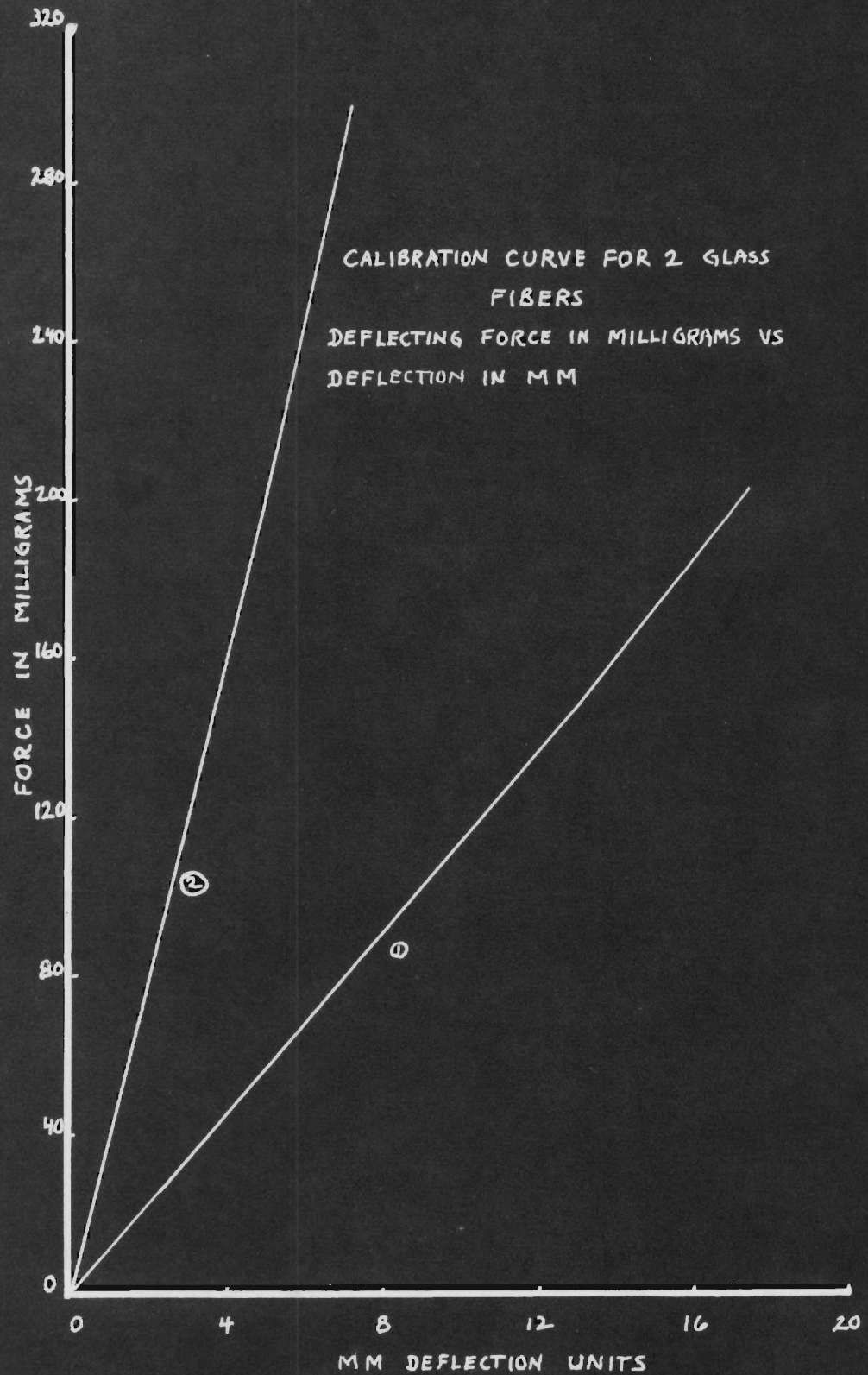


fig 16

$F_R$  can now be expressed as a function of  $F_F$  in Equation (25)

$$\bar{E} = \frac{.278 F_F}{2} = .0197 F_F \quad (27)$$

$$\bar{E} = (.0197)(.160)(980) = 3.08 \frac{\text{ergs}}{\text{cm}^3} \quad (28)$$

To convert the expressions for the energy density into intensity, the fundamental relation below is given,

$$\bar{I} = \bar{E} v \quad \text{where } v \text{ is the velocity of sound}$$

For the spheres, taking  $v = 144,000 \text{ cm/sec}$ ,

$$\bar{I}_1 = \bar{E}_1 v = (3.54)(144,000)(10^{-7}) = .047 \frac{\text{watts}}{\text{cm}^2}$$

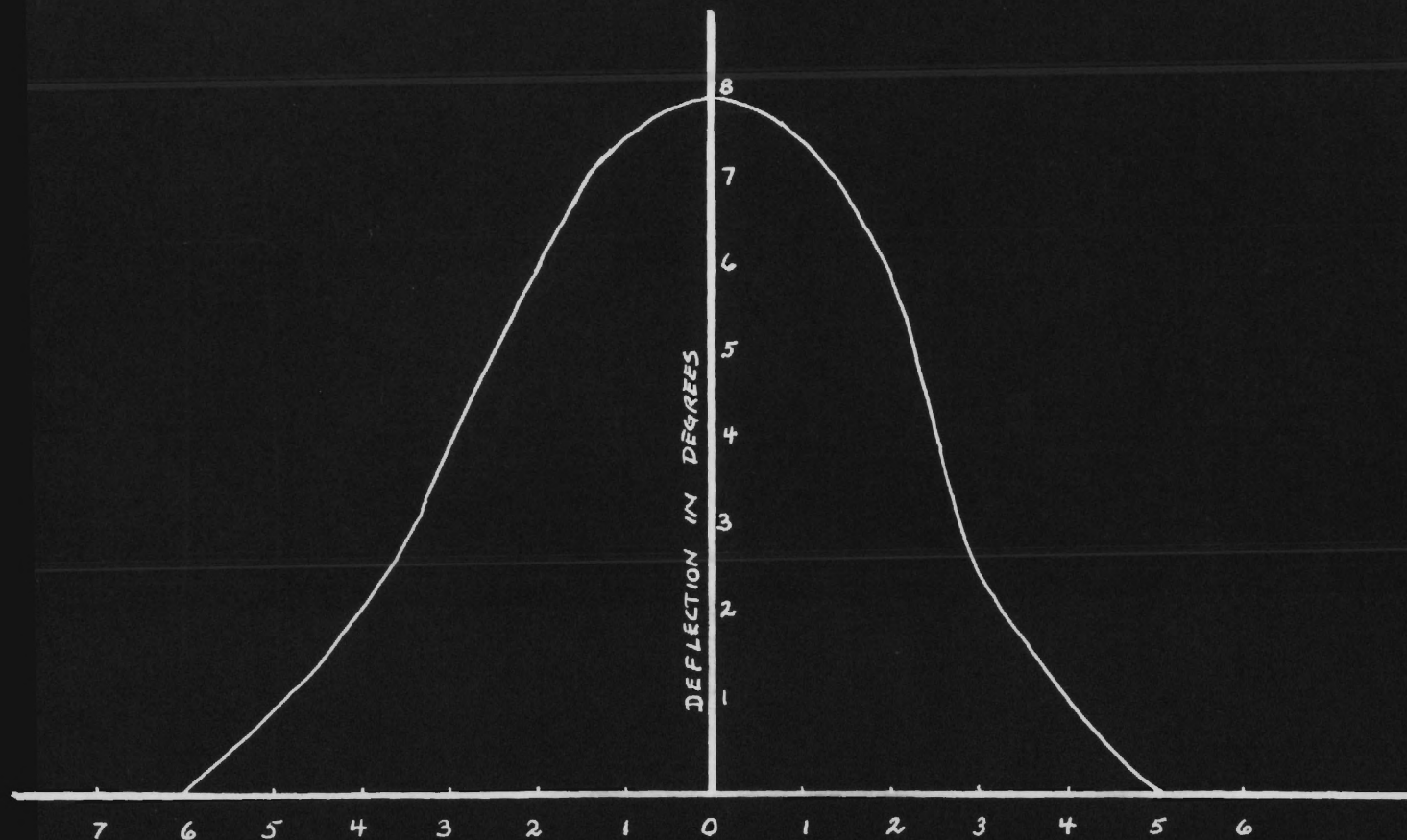
$$\bar{I}_2 = \bar{E}_2 v = (45.0)(144,000)(10^{-7}) = .65 \frac{\text{watts}}{\text{cm}^2}$$

and for the air vane,

$$\bar{I} = \bar{E} v = (3.08)(144,000) = .045 \frac{\text{watts}}{\text{cm}^2}$$

The value of the field produced by the transducer as measured by the large sphere and the vane agree to four per cent while a discrepancy by a factor of more than ten exists between this value and that obtained by the small sphere. This can be explained by examination of the curve in Figure 17 showing a typical cross-section of the beam. A fairly sharp maximum occurs in the center of the beam and the large difference in the diameter of the measuring devices would give different average intensities. The larger value for the small sphere is consistent with this if one





CM FROM CENTER OF BEAM  
A TYPICAL CROSS SECTION OF THE BEAM AT  
A DISTANCE OF 30 CM FROM THE TRANSDUCER

Figure 17

assumes it was placed in the center of the beam. The relative maximum errors for this series of measurements is given in Appendix IV.

#### Measurement by the Copper Sulfate Probe

The order of magnitude of the expected signal can be estimated from the preceding data.

Let  $p$  equal pressure amplitude;  $I$ , intensity;  $v$ , velocity of sound;  $k$ , compressibility;  $\rho$ , density of the medium, all expressed in absolute units, then,

$$I = v 2^{\frac{1}{2}} k p^2 \frac{\text{dyne}}{\text{cm sec}} \quad (29)$$

and as

$$v = \sqrt{\frac{1}{\rho k}} \quad (30)$$

$$I = \frac{p^2}{\rho v}$$

$$p = (\rho v I)^{\frac{1}{2}} \text{ as } v = 144,100 \frac{\text{cm}}{\text{sec}} \quad (31)$$

$$\rho = 1 \text{ gm/cm}^3$$

then converting to atmospheres,

$$p = 1.2 (I)^{\frac{1}{2}} \text{ atm.} \quad (32)$$

For the measurement using the vane,

$$p = 1.2 (.04)^{\frac{1}{2}}$$

$$p = .24 \text{ atm.}$$

assume 1/4 volt, 1000 c.p.s. signal,

$$E_s = 115 \text{ microvolts per atm. per applied volt}$$

$$= 5.5 \text{ microvolts}$$

s = side band

and for both side bands,

$$E_{\text{total}} \approx 10 \text{ microvolts}$$

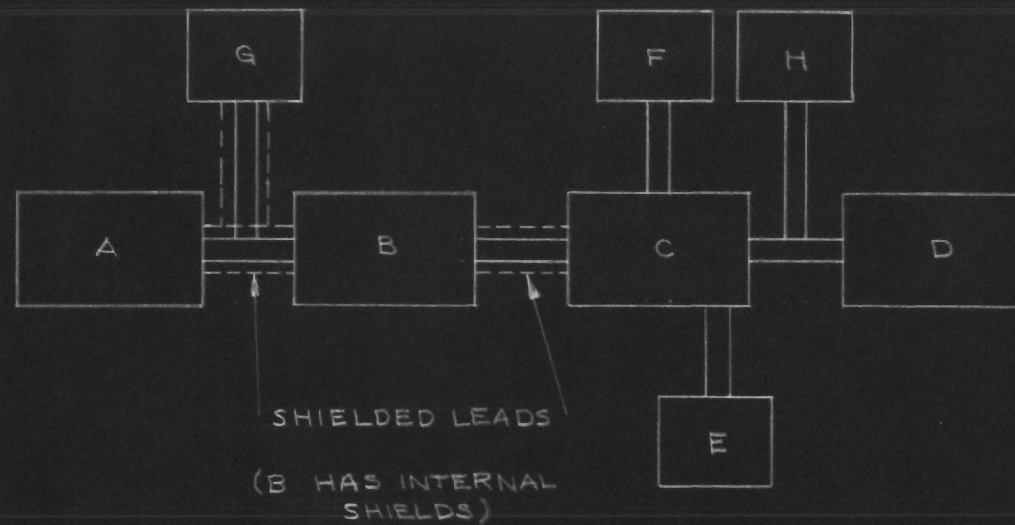
As the order of magnitude of the signal was not much above the expected noise level of the tubes, care was exercised to shield all important leads to the amplifier. The probe itself was completely shielded except for the electrodes as shown in Figure 6.

The procedure involved in determining the input signal corresponding to a given output for the feedback amplifier is outlined below, with reference to the block diagram of Figure 19.

- A. A line voltage regulator was used with the power supply to the amplifier to minimize disturbances due to fluctuations of the line voltage.
- B. The chassis of the amplifier was used to ground all other equipment.
- C. The audio oscillator, the source of the 50 kc signal, was operated for 30 minutes before any readings were taken. Shielded leads were used to the attenuator and from the attenuator to the amplifier.
- D. A 600 ohm termination was provided on the audio oscillator end of attenuator and a 1000 ohm termination on the amplifier end.
- E. A signal was put in from the audio oscillator with the



BLOCK DIAGRAM OF APPARATUS USED IN CALIBRATION OF  
HI-SENSITIVITY CONSTANT GAIN - VOLTAGE AMPLIFIER



A - HEWLETT PACKARD AUDIO OSCILLATOR

B - 600  $\Omega$ -T PAD G.R. ATTENUATOR

C - HI SENSITIVITY, CONSTANT GAIN VOLTAGE AMPLIFIER

D - HICKOK A.C. V.T.V.M.

E - G.R., D.C. VOLTMETER

F - REGULATED POWER SUPPLY

G - G.R., V.T.V.M.

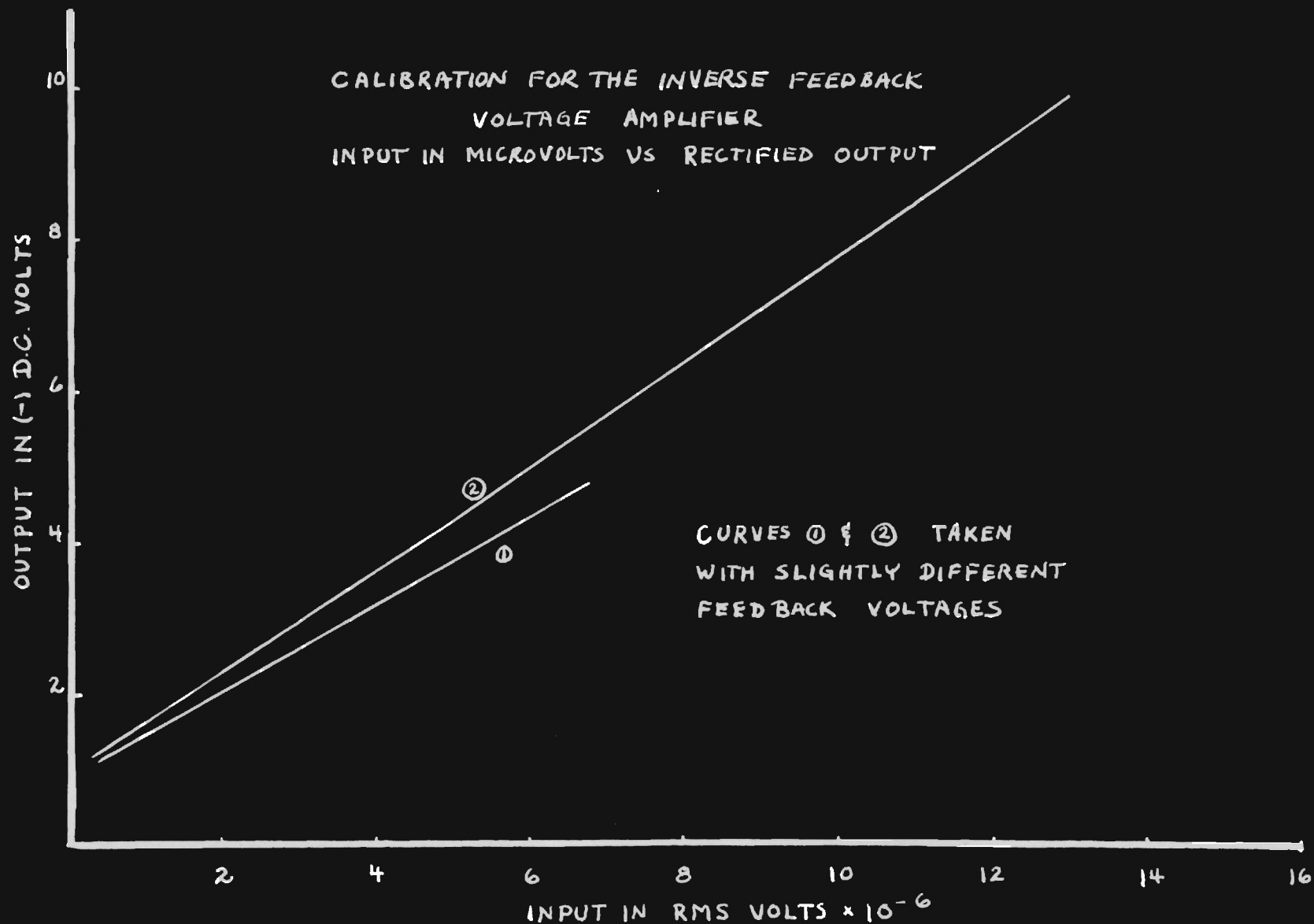
H - DUMONT OSCILLOSCOPE

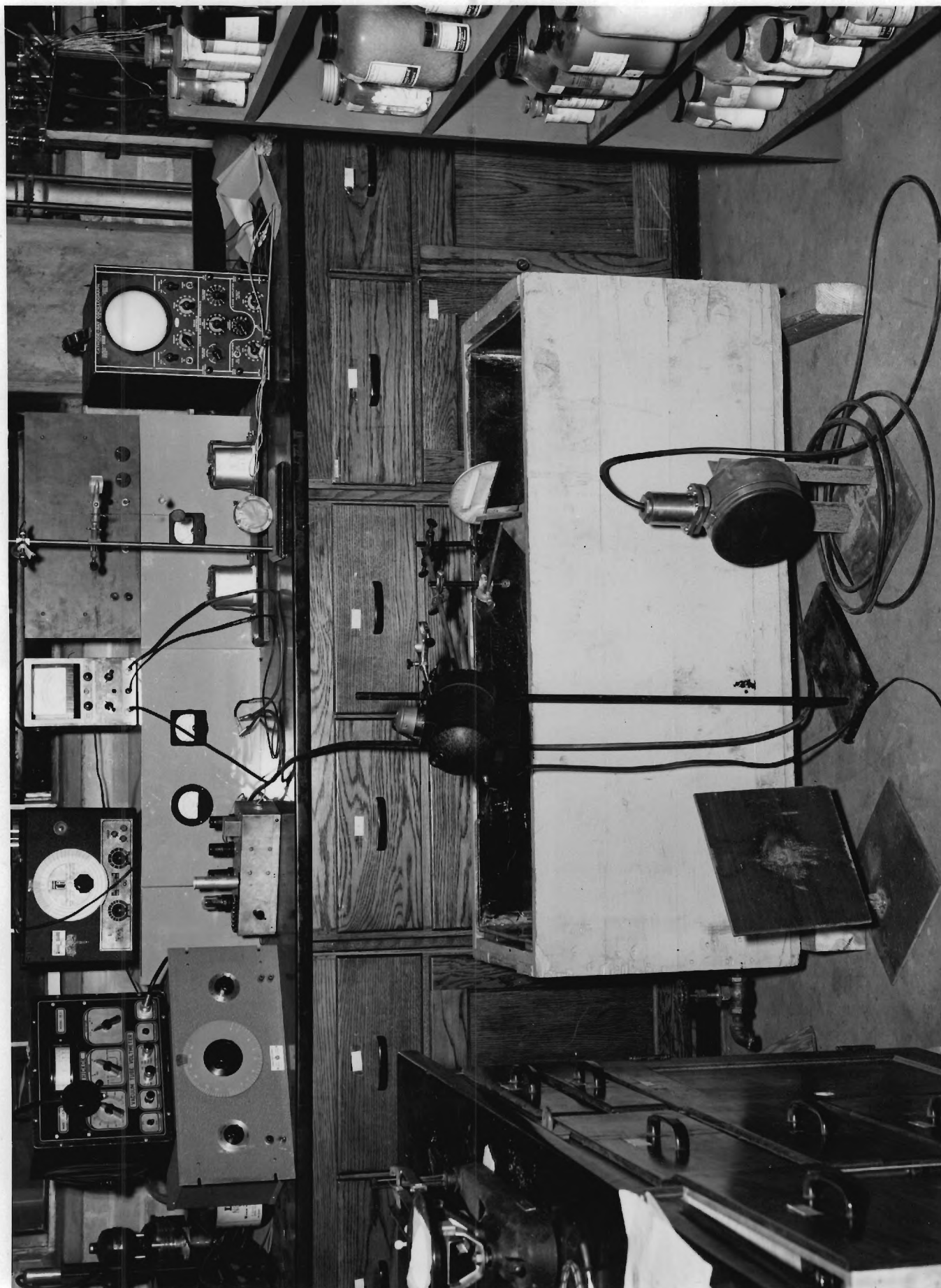
Figure 19

feedback control at zero volts. The output was adjusted to give one volt and the feedback then increased until this reading was reduced to one half volt. This determined the setting of the feedback control. It was observed that if the feedback was increased by the same amount the amplifier began to oscillate at a high frequency of the order of 300 kc. This was true even with the input shorted at the attenuator. However, by operating below this region there was no observed tendency to oscillate.

- F. When the input to the amplifier was shorted, and with the plate and filament voltages applied, a DC output from the rectifier of -1.1 volts was observed. This was attributed to the thermal electron current through the rectifier tube. The rectifier was operated to produce a negative DC voltage.
- G. The signal began to appear in the output as observed on the oscilloscope when its magnitude was of the order of one microvolt.
- H. The plate voltage to the amplifier was adjusted for 250 volts and a considerable variation in amplification was observed as the plate voltage was varied from 200 to 300 volts. The plate voltage was adjusted to 250 volts and this setting remained fixed for all of the subsequent work.

The calibration curves, Figures 20 and 21, show the AC and DC output of the amplifier versus the input in microvolts for two slightly different settings of the feedback. The curves are sufficiently linear to allow accurate extrapolation between calibration points.





Photograph of the Apparatus

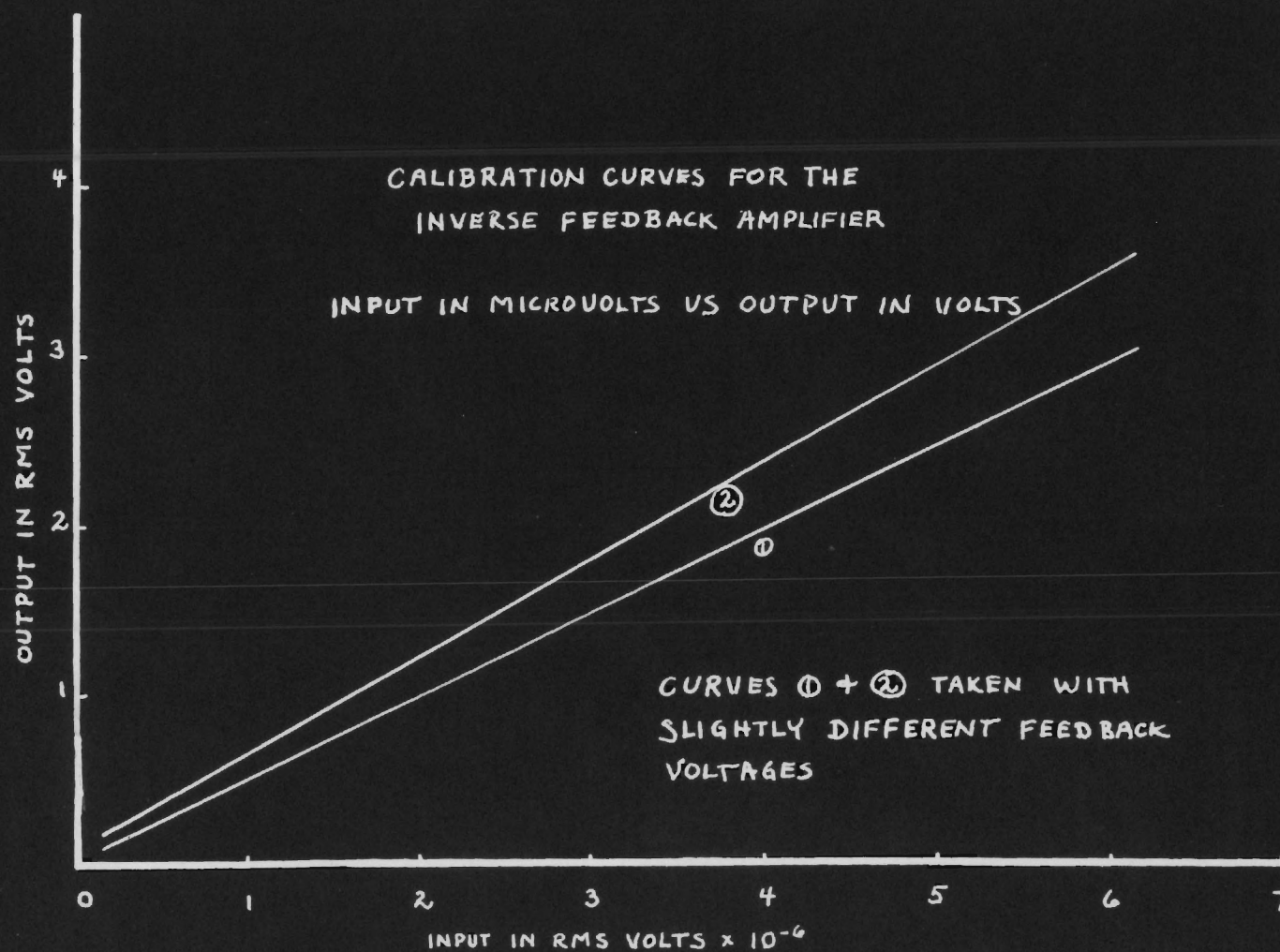


Figure 21

The amplifier was mounted directly above the tank in order to make the lead from the probe to the amplifier as short as possible. A wire was dropped into the water, thus grounding the water and the chassis of the amplifier, and likewise, the chassis was grounded to the driving unit of the transducer and to a water pipe. With no B+ applied to the transducer driving unit, the output of the feedback amplifier was 1.4 volts due to the thermal electrons. The audio oscillator furnishing the 1000 c.p.s. constant current was turned off when the B+ was turned on to the driving unit. A large signal at the frequency of the driving unit was amplified by the inverse feedback amplifier, and the rectified signal was 30 volts or more.

At first this signal was thought to be due to the sound, even though there should be no output when the constant current source was turned off and these terminals shorted. To examine this possibility the following tests were made:

- A. If the probe was removed from the water, but electrical contact was maintained by allowing the brass ring to make contact, the signal would disappear.
- B. The probe was left in the water and the transducer removed. If the transducer were completely removed the signal disappeared, but if the iron stand were touched to the water, it would gradually reappear as more and more of the transducer was submerged.
- C. A glass beaker was submerged in the water, with both probe and transducer immersed, and as the beaker was slipped over the probe the signal would decrease to zero.



- D. When different substances were placed between the transducer and the probe, only slight changes in the signal could be detected. The signal would vary as the position of the transducer with respect to the probe was changed, and if the transducer was pointed away from the probe, a slight change downward would occur. This was much less, however, than should be expected if the probe were detecting sound energy.
- E. No significant change in the signal occurred when the 1000 c.p.s. source was turned on. As the amplitude of the 1 kc signal was increased, a slight increase in the output was noticed, but when the amplitude was of the order of .2 volt the amplifier broke into oscillations.
- F. The reflector plate was placed in the tank opposite the transducer, and, as the probe was moved back and forth between the plate and transducer, maxima and minima were superimposed on an increasing signal as the probe was moved towards the transducer. This behavior indicated a system of standing waves some  $3\frac{1}{2}$  to 5 cm wave length.

From these tests, there is evidence of two effects, one due to sound, and the other due to radiation of an electromagnetic 50 kc signal from the driver unit. Analysis of each test follows:

- (A) would indicate that the signal was due to sound waves;
- (B) would indicate that there was sound conducted from the transducer through the iron stand to the water. This is a possibility but the magnitude of the signal was such that just as much sound would appear to come from the stand

as from the transducer;

- (C) indicates evidence of the presence of a sound field;
- (D) shows the attenuation by a plate of glass to be of the order of five per cent, but it should be of the order eighty-five per cent. The lack of directivity indicated an absence of a sound field;
- (E) shows the slight change in signal when the 1 kc source was turned on and could be attributed to sound energy or amplification of the high harmonics of the 1 kc signal;
- (F) seems to indicate the presence of standing waves, even though of the wrong wave length.

In order to have the electromagnetic phenomenon without the sound energy, the high voltage lead to the transducer was disconnected. Tests (A) through (E) were repeated and exactly the same behavior was observed to occur. Furthermore, as the probe was moved up and down and across the tank while under water, widely different signals were observed. If removed from the water, the signal went down below the noise level. This then partially explained some of the behavior but left unsolved the reason for (A), (C), and (F).

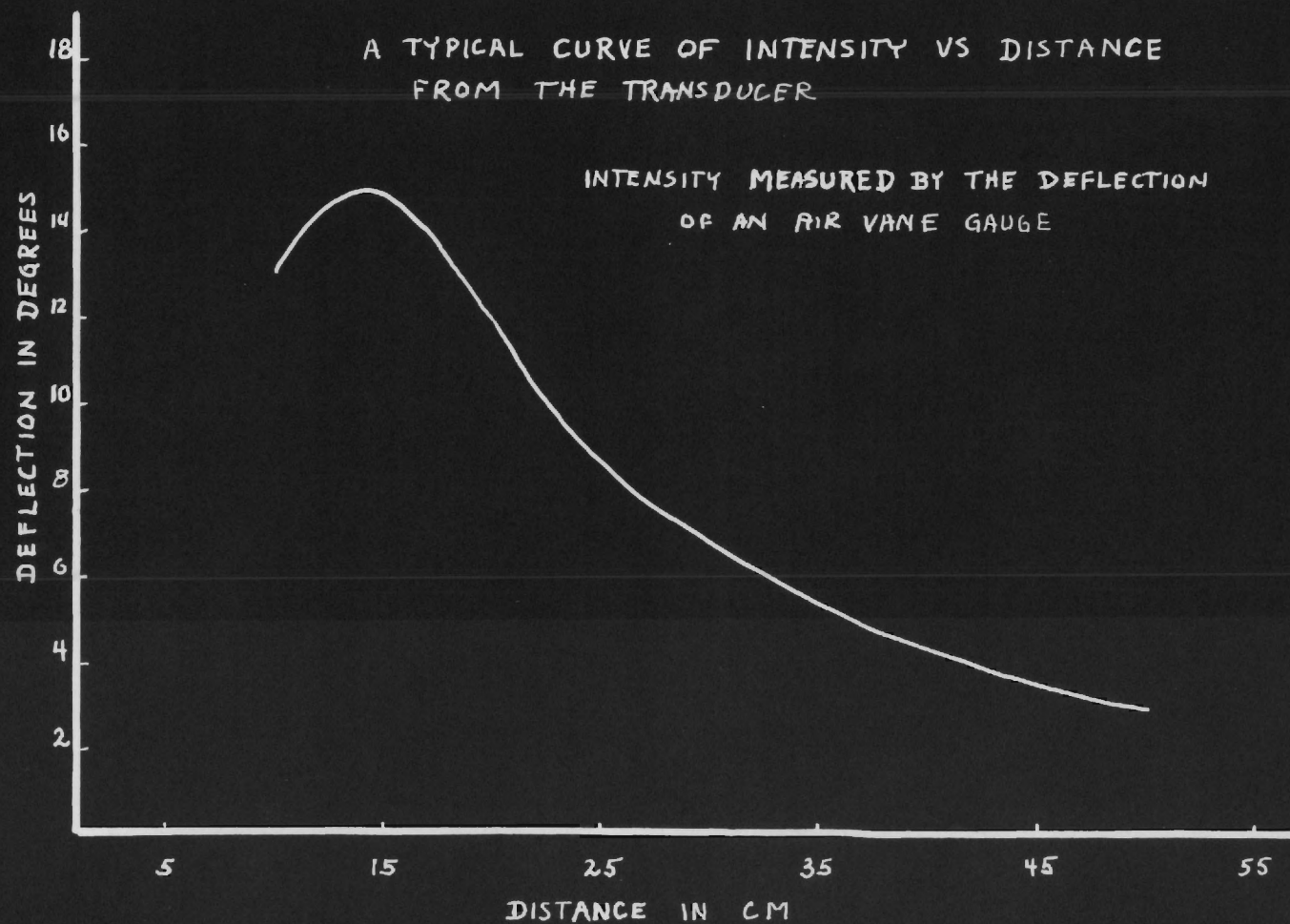
Subsequent rearrangement of the ground leads and complete shielding reduced the pick-up to 15 volts output. A small change in this, due to a sound field, was observed, but this effect could not be reproduced with the same magnitude for a given field.



## SECTION IV

## PROPERTIES OF THE SOUND FIELD AND MISCELLANEOUS GRAPHS

This section contains Graph 1, A Plot of the Field Strength as a Function of the Distance from the Transducer; Graph 2, Frequency Response of the Transducer for a Constant Input Voltage; Graph 3, Output of the Transducer as a Function of Input Voltage at Constant Frequency; and Graph 4, Calibration Curve of Input Voltage Versus Output Voltage for the Power Amplifier Unit. This section also includes a reference diagram for Appendix IV and a photograph of the apparatus.

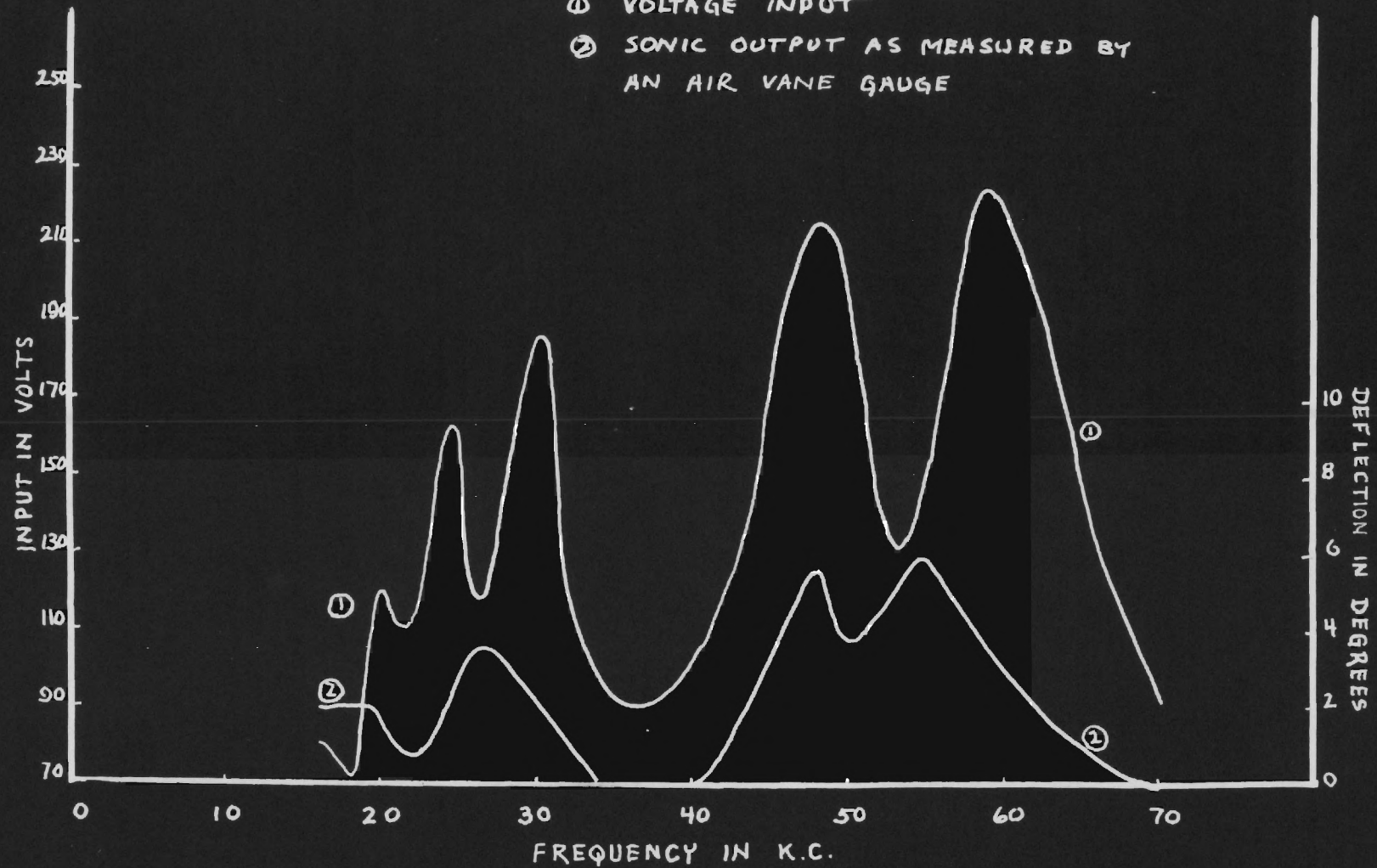


Graph 1

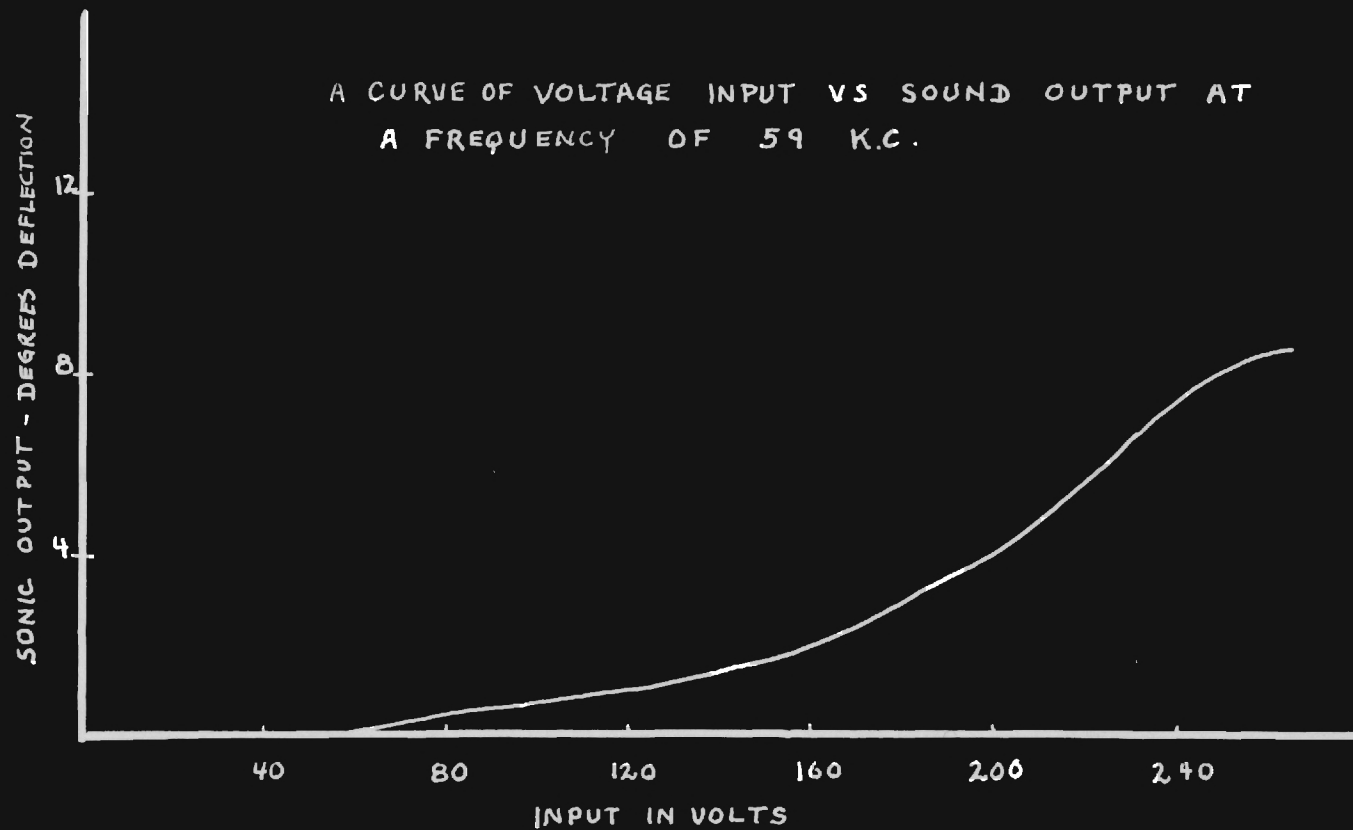
TWO CURVES SHOWING FREQUENCY  
CHARACTERISTICS OF THE TRANSDUCER

① VOLTAGE INPUT

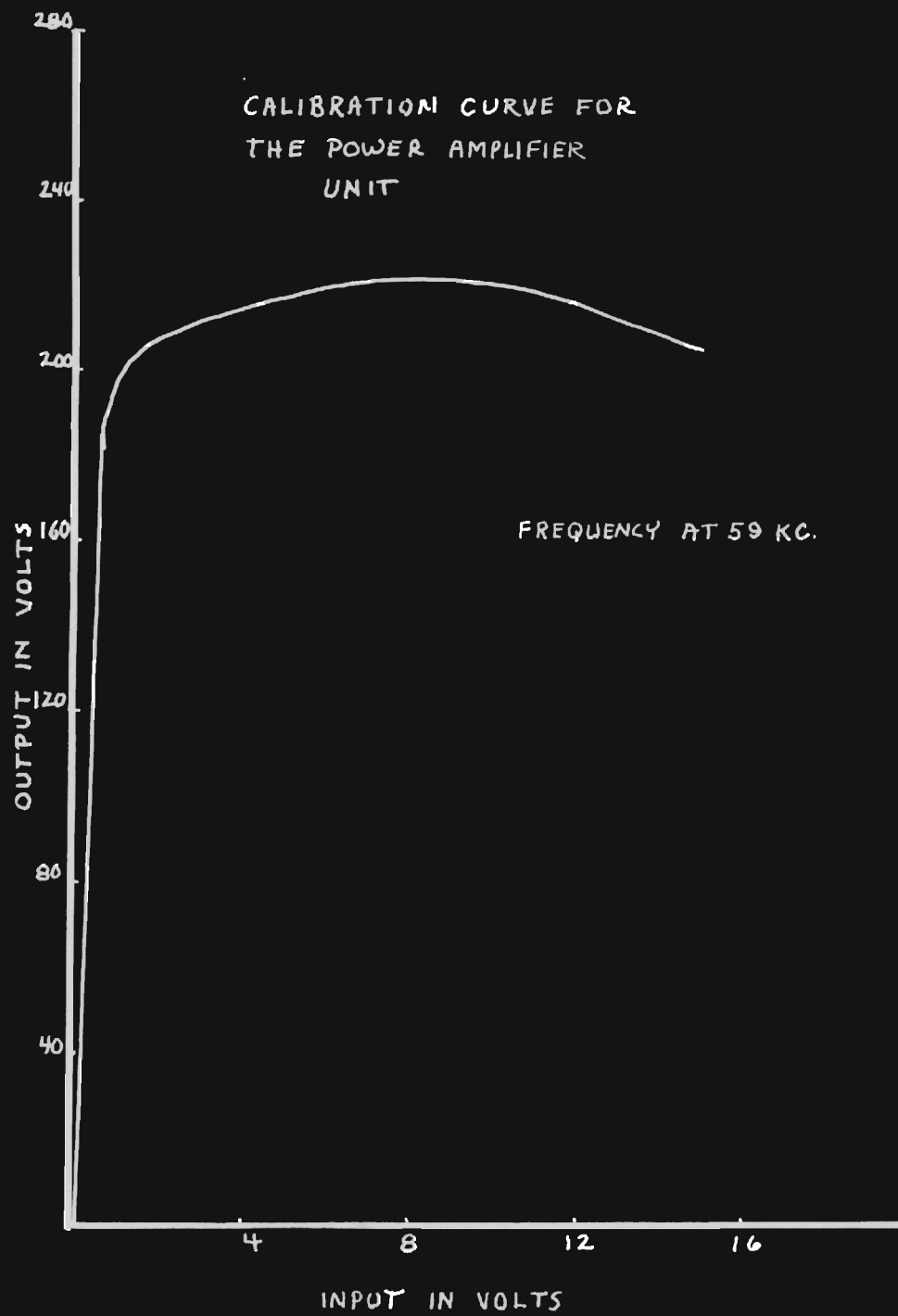
② SONIC OUTPUT AS MEASURED BY  
AN AIR VANE GAUGE



Graph 2

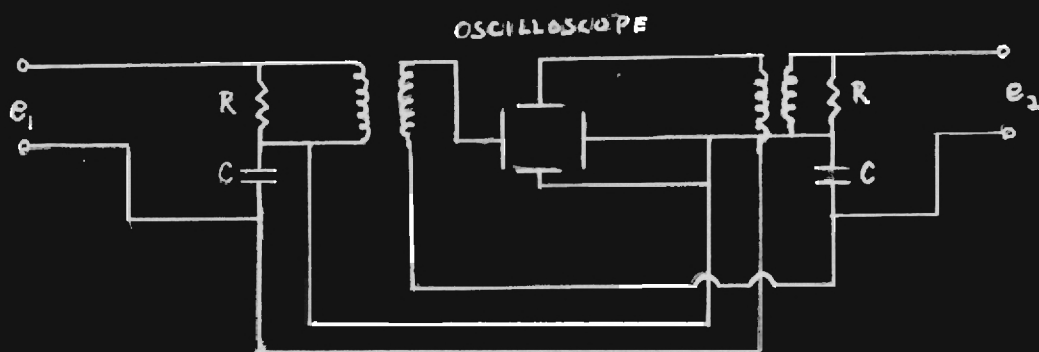


Graph 3

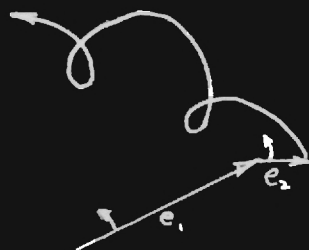


Graph 4

# REFERENCE DIAGRAMS FOR APPENDIX IV

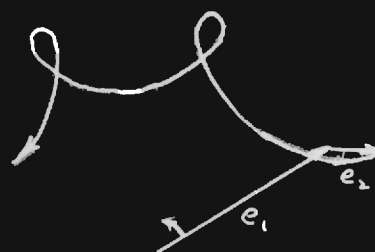


$$f_{e_2} = (n+1) f_{e_1}$$



A

$$f_{e_2} = (n-1) f_{e_1}$$



B

## SUMMARY

An ultrasonic field was generated at 50 kc by driving an ammonium phosphate crystal transducer and absolute measurement of the field strength indicates an average value of  $.046 \frac{\text{watts}}{\text{cm}^2}$  for 215 volts input to the transducer. The properties of the sound field are investigated and shown on graphs. A method of measurement of the field using a  $\text{CuSO}_4$  probe failed to give reliable results due to difficulty experienced in shielding the measuring equipment from stray signals.

## APPENDIX I

## THEORY OF FOX METHOD FOR MEASURING ABSOLUTE SOUND INTENSITY

Investigations involving the determination of absolute and relative intensities of acoustic waves in liquids by radiation pressure measurements have made it desirable to have available the values of the constant relating the radiation pressure in a sphere to the sound intensity in the medium. King<sup>9</sup> has developed formulas including the case for the radiation pressure of plane progressive sound waves in a frictionless medium upon rigid spheres. The radiation pressure is expressed as a function of the intensity (or a quantity related to the velocity potential) of the sound, the relative densities of the sphere and the medium, and a parameter  $\alpha = 2\pi r/\lambda$  where  $r$  is the radius of the sphere and  $\lambda$  is the acoustic wave length in the liquid. For  $\alpha \leq 1$  the calculations are relatively simple but for larger values of  $\alpha$  they become more and more tedious, involving many terms of a series containing Bessel Functions of large argument and high odd half-integer orders. These in turn must be calculated by series or by extending existing tables by means of recurrence formulas to higher values of the order.

The theory is to be used in experimental work in this laboratory and it was planned to carry the investigation to as high a frequency as feasible, and, since for a given sphere the parameter  $\alpha$  increases with the frequency, it becomes evident that it would be of advantage to have some means of quickly determining the radiation pressure constants for any value of  $\alpha$ . Different spheres could be selected for different frequencies so that the  $\alpha$  remains constant but technical considerations make



this impracticable. It seemed simpler to compute the constants for a number of integer values of  $\alpha$  and then interpolate. Further, it is possible to find a simple extrapolation formula for very large  $\alpha$ .

### Methods

King gives the mean radiation pressure on a sphere in a plane progressive wave,

$$P = (2\pi p_0 |A|^2 / \alpha^2) \left[ (1/H_0^2 H_1^2) + (2/H_1^2 H_2^2 \alpha^8) \{ \alpha^2 - 3(1 - p_0/p_1) \}^2 + \sum_{n=2}^{\infty} \left\{ (n+1)/H_n^2 H_{(n+1)}^2 (4n+4) \{ \alpha^2 - n(n+2) \}^2 \right\} \right] \quad (1a)$$

which may be written as

$$\bar{P} = p_0 |A|^2 F \quad (1b)$$

in which  $F$  is the function of  $\alpha$  and  $p_0/p_1$  to be evaluated where  $p_0$  = the density of the medium,  $p_1$  = the density of the sphere,  $\alpha = 2\pi r/\lambda$ ,  $r$  = radius of sphere,  $\lambda$  = acoustic wave length in the medium, and  $A$  is the coefficient associated with the velocity potential of the incident radiation field defined as that the mean total energy density in the wave is  $E = p_0 k^2 |A|^2 / 2$  where  $k = 2\pi/\lambda = \omega/r$ .

The  $H_n$  are further defined,

$$H_n^2 = (\pi/2 \alpha^{2n+1}) \left[ n^2 (J_{(n+\frac{1}{2})}^2 + J_{(-n-\frac{1}{2})}^2) + 2n\alpha (J_{(-n-\frac{1}{2})} J_{(-n-3/2}) - J_{(n+\frac{1}{2})} J_{(n+3/2)}) + \alpha^2 (J_{(n+3/2)}^2 + J_{(-n-3/2)}^2) \right], \text{ for } n \neq 1 \quad (2a)$$

and,

$$H_1^2 = (\pi/2 \alpha^3) \left[ (1 - p_o/p_1)^2 (J_{3/2}^2 + J_{-3/2}^2) + 2\alpha(1 - p_o/p_1)(J_{-3/2} J_{-5/2} - J_{3/2} J_{5/2}) + \alpha^2 (J_{5/2}^2 + J_{-5/2}^2) \right]$$

In all these the Bessel Functions  $J_{\pm(n+1/2)}$  are of argument  $\alpha$ .

It is possible, moreover, to express the  $H_n^2$  as polynomials and this is of special interest when dealing with spheres for which  $\alpha \leq 1$ , where only the first two terms in (1a) are needed to obtain  $F$  with an accuracy of better than 1 per cent. These are given here to collect all the formulas necessary for the computations for any  $\alpha$ .

$$H_0^2 = (1 + \alpha^2)/\alpha^2 \quad (2b)$$

$$H_1^2 = (4/\alpha^6) \left[ (1 + p_o/2p_1)^2 + (\alpha^2/2)(1 + p_o/2p_1)(p_o/p_1) + \alpha^4/4 \right],$$

$$H_2^2 = (81/\alpha^{10}) \left[ 1 + (\alpha^2/9) - (2\alpha^4/81) + \alpha^6/81 \right].$$

King points out that for  $\alpha \ll 1$  it is sufficient to take the first two terms in (1a), so that

$$F \cong 2 \pi \alpha^6 \left[ 1 + 2(1 - p_o/p_1)/9 \right]^2 / (2 + p_o/p_1)^2 \quad (3)$$

The neglected terms contain  $\alpha$  in the eighth or higher powers.

If we take  $\alpha = 1$  the error in neglecting the third term is still small, i.e., less than one per cent, and that

$$F \cong (\pi/89) \left[ 105 - 48(p_o/p_1) + 36(p_o/p_1)^2 \right] / \left[ 5 + 6(p_o/p_1) + 2(p_o/p_1)^2 \right] \quad (4)$$

The results of the calculation for values of  $\alpha = 1$  to 11, and 15 and 20 are given in Table I for values of  $p_o/p_1 = 1, 0.5, 0.2, 0.1$ , and 0.

For  $\alpha > 1$  the series for  $F$  was carried out till the remainder terms were negligible.  $F$  for  $\alpha = 20$  includes e.g. 26 terms and necessitated the calculation of  $H_n^2$  to  $n = 26$ , with the Bessel functions  $J_{\pm 57/2}(20)$ . For the Bessel functions eight places were taken from a twelve-place table,<sup>10</sup> and the tables were extended, to include the order needed, by the recurrence formula,

$$J_{n+1}(\alpha) + J_{n-1}(\alpha) = (2n/\alpha) J_n(\alpha) \quad (5)$$

It is evident that  $F$  is approaching the limiting value  $\pi\alpha^2/2$  as  $\alpha \rightarrow \infty$  and this suggests dividing  $F$  by  $\pi\alpha^2/2$ . Setting  $Y = 2F/\pi\alpha^2$  it is seen that  $Y$  approaches 1 as  $\alpha$  increases and is useful if one wants to express  $P$  through  $E$ . Thus we may write (5) as

$$P = Y E(\pi r^2) \quad (6)$$

### Results

The values of  $F$  are given in Table I,  $Y$  in Table II.

### Conclusion

The calculations necessary to obtain constants relating radiation pressure of a plane progressive wave on a sphere to the acoustic energy density in the medium have been made so that one may with relative ease obtain the constants for all values of  $\alpha = 2\pi r/\lambda$  from 0 to  $\infty$  with an accuracy of better than one per cent.

TABLE I

F as Defined by Eq. (1) for Various Values of  $\alpha$  and  $p_0/p_1$ . The values of  $\pi\alpha^2/2$  are given for comparison

$\alpha$	$\pi\alpha^2/2$	F				
		$p_0/p_1 = 0.0$	0.1	0.2	0.5	1.0
1	1.571	0.7439	0.6342	0.5469	0.3764	0.2551
2	6.283	4.725	4.650	4.608	4.609	4.967
3	14.14	11.68	11.93	12.16	12.79	13.57
$\pi$	15.50	12.94	13.19	13.42	14.04	14.78
4	25.13	21.79	21.98	22.16	22.61	23.07
5	39.27	35.07	35.21	35.33	35.63	35.89
6	56.55	51.53	51.63	51.71	51.92	52.09
7	76.97	71.16	71.23	71.29	71.45	71.56
8	100.5	93.95	94.01	94.06	94.17	94.26
9	127.2	119.9	120.0	120.0	120.1	120.2
10	157.1	149.0	149.1	149.1	149.2	149.2
11	190.1	181.3	181.3	181.4	181.4	181.5
15	353.4	342.0				342.1
20	628.3	613.8				613.9

TABLE II

The Values of  $Y = 2F/\pi\alpha^2$  for F Given in Table I

$\alpha$	Y				
	$p_0/p_1 = 0.0$	0.1	0.2	0.5	1.0
1	0.4736	0.4038	0.3482	0.2396	0.1624
2	.7521	.7401	.7335	.7335	.7906
3	.8261	.8437	.8604	.9054	.9612
$\pi$	.8347	.8507	.8658	.9055	.9534
4	.8670	.8748	.8819	.8997	.9180
5	.8931	.8966	.8997	.9072	.9141
6	.9113	.9130	.9145	.9182	.9212
7	.9245	.9254	.9257	.9282	.9298
8	.9346	.9351	.9356	.9368	.9376
9	.9424	.9428	.9431	.9438	.9443
10	.9488	.9490	.9492	.9497	.9500
11	.9540	.9541	.9542	.9546	.9548
15	.9677				.9679
20	.9769				.9770

## APPENDIX II

THEORY OF FOX, HERTZFELD AND ROCK METHOD FOR MEASURING  
ABSOLUTE SOUND INTENSITY

Static measurements of the effect of pressure on the conductivity of salt solutions have been made by Koerber.<sup>11</sup> In the range of pressures below 1000 atmospheres, he finds an increase in conductivity proportional to the pressure. A maximum occurs near 1200-1500 atmospheres.

Koerber has found that for simple, monovalent salts like sodium and potassium chloride, the effect is nearly independent of the concentration of the solution and alike for the two salts.

At 19.18° C., the change of resistance between 0 and 500 atmospheres is found to be 3.7 per cent, which means that the relative conductivity increase is  $74 \times 10^{-6}$  per atmosphere. This value agrees well with a calculation founded on the assumption that two effects contribute to the increase of conductivity: the decrease of viscosity with pressure,<sup>12</sup> and the increase of the concentration, due to compression.

At 0.01° C., only measurements for 0.01 n-potassium chloride solutions have been made. They give a relative increase in conductivity of  $98 \times 10^{-6}$  per atmosphere.

Koerber did not measure copper sulphate, but he measured zinc sulphate, which behaves electrolytically very similarly to copper sulphate. Therefore, it seems reasonable to assume that the dependence of conductivity on pressure will be similar for the two salts.

For  $\text{ZnSO}_4$  the effect is found to be dependent on the concentration, contrary to the behavior of sodium chloride, and to be larger than in the former case.

This can be explained on the basis that the apparent dissociation of divalent salts like copper sulphate and zinc sulphate is not complete and is increased by pressure.

The increase of conductivity for 0.2 normal zinc sulphate is, at 19.18° C., 10 per cent for 500 atmospheres, or  $200 \times 10^{-6}$  atmosphere.<sup>13</sup> No measurements exist near 0° C.

These measurements are for a static application of pressure. In a sound wave, or shock wave traveling in water, pressure rise is accompanied above 4° C. by a temperature rise, which diminishes the viscosity and increases the conductivity.

The increase  $\Delta T$  in temperature is connected with the increase  $\Delta p$  in pressure by the following formula.<sup>14</sup>

$$\frac{\Delta T}{\Delta p}_s = \frac{T}{C_p} \left( \frac{\partial V}{\partial T} \right)_p = \frac{T V}{C_p} \frac{1}{V} \left( \frac{\partial V}{\partial T} \right)_p \quad (1)$$

Here,  $(\partial V/V \partial T)_p$  is the usual coefficient of heat expansion, and  $C_p/V$  the specific heat of unit volume.

One finds in Table I results for the temperature increase per atmosphere.

TABLE I

Calculated Increase of Temperature in Water Per Atmosphere Adiabatic Pressure Increase, and Relative Increase in Conductivity

t =	0	2.5°	4°	5.5°	10.5°	15.5°	20.5°
$\Delta t^{\circ}\text{C} \times 10^{-3}$	-0.38	-0.16	0	0.16	0.64	1.1	1.5
Relative conductivity increase $\times 10^{-6}$	-13	-5	0	5	18	28	37

These values are applicable to both sodium chloride and copper sulphate. At 20° C. an increase of conductivity per atmosphere, adiabatically applied, of  $(74 + 37) \times 10^{-6} = 110 \times 10^{-6}$  for sodium chloride, and of  $(200 + 37) \times 10^{-6} = 235 \times 10^{-6}$  for 0.2 normal copper sulphate is expected. At 0° C. one should expect  $(94 - 13) \times 10^{-6}$  or  $81 \times 10^{-6}$  for 0.01 n-sodium chloride solution. It cannot be decided whether the small dependence on concentration would materially affect the dependence on temperature.



## APPENDIX III

PROCEDURE USED IN OBTAINING AN ACCURATE FREQUENCY RESPONSE  
CURVE FOR THE TRANSDUCER

The 60 cycle commercial power was selected as a frequency standard by which a Hewlett-Packard audio was set to 1000 cycles/sec. The procedure is explained below.

The circuit shown in Section IV was employed. The 60 cycle commercial voltage was used for  $e_1$ . The output of a Hewlett-Packard audio oscillator served as  $e_2$ . With  $e_2$  set equal to zero and with  $e_1$  equal to 6.3 volts,  $R_1$  was adjusted until there was a  $90^\circ$  phase difference between voltages applied to the horizontal and vertical deflecting plates. For this condition the trace on the oscilloscope was a circle. The gain on the oscilloscope was adjusted for a circle approximately two and one half inches in diameter. With  $e_1$  set to zero and  $e_2$  approximately 3 volts,  $R_2$  was adjusted for a circular trace on the oscilloscope. The output of the audio oscillator was adjusted for a circle whose diameter was approximately one half inch.

Both voltages were applied and the frequency of the audio oscillator was adjusted for the stationary pattern as shown in the figure in Section IV. The frequency of the voltage  $e_2$  is one more than the number of external cusps multiplied by frequency of  $e_1$ .

For this calibration the frequency of  $e_2$  was adjusted for a roulette pattern with nine external cusps, that is 600 cycles/sec. The commercial power was disconnected and the output of the driver was applied for  $e_1$ . With the frequency of  $e_2$  still set on 600 cycles/sec., the driver oscillator frequency was adjusted to 6000 cycles/sec. The frequency of

the audio oscillator,  $e_2$ , was then set to 1000 cycles/sec. and maintained constant.

This now furnished a 1000 c.p.s. frequency standard. Using this frequency standard, roulette figures containing up to 70 cusps could be accurately counted. It was then possible to proceed in steps of 1 kc from 16 kc to 70 kc and thus obtain an accurate response curve.

## APPENDIX IV

## ESTIMATION OF MAXIMUM RELATIVE ERROR

For the spheres,

$$I = \frac{k^2 F \tan \theta v}{2F(\varphi) \pi \kappa^2}$$

$$\ln I = 2 \ln k^2 + \ln F + \ln \tan \theta + \ln v - \ln 2 - \ln F(\varphi) - \ln \pi - 2 \ln \kappa$$

The maximum relative error,

$$\frac{dI}{I} = \frac{dF}{F} + \frac{\sec^2 \theta}{\tan \theta} d\theta + \frac{dv}{v} - \frac{dF(\varphi)}{F(\varphi)} - 2 \frac{d\kappa}{\kappa}$$

Values for Sphere #1,

$$\frac{dI}{I} = \frac{1}{300} + \frac{1}{.013} .003 + \frac{.3}{144} - .01 - 2 \frac{.001}{.8} = .25$$

and for Sphere #2,

$$\frac{dI}{I} = .03 + \frac{1}{.026} .003 + .02 - .01 - 2 \frac{.001}{.23} = .15$$

For the vane,

$$I = \frac{L_F}{L_R} F_F v \quad \ln I = \ln L_F + \ln F_F + \ln v - \ln L_R$$

$$= \frac{.05}{3.5} + \frac{4}{150} + .02 - \frac{.05}{13}$$

$$= .037$$

Table I

## Physical Properties of the Two Spheres

Sphere #1		Sphere #2	
Diameter cm		Diameter cm	
0° Longitude	90° Longitude	0° Longitude	90° Longitude
1.6291	1.6240	.5510	.5778
1.6316	1.6205	.5770	.5347
1.6200	1.6185	.5839	.5344
1.6188	1.6216	.5844	.5845
1.6182	1.6380	.5843	.5868
1.6195	1.6378	.5832	.5852
1.6240	1.6228	.5836	.5860
		.5790	.5860
		.5504	.5880

Wt. = 2.852 gms.

Wt. = .131 gms.

## Diameter of Supporting Fiber

At Bead - .0285 cm  
 Mid-Point - .0289 cm  
 At End - .0240 cm

At Bead - .0100 cm  
 Mid-Point - .0216 cm  
 At End - .0232 cm

Length of Suspension of Sphere #1 and #2 = 13.5 cm

Ave. Diameter - 1.6246 cm  
 Ave. Radius - .8123 cm

Ave. Diameter - .5810 cm  
 Ave. Radius - .2905 cm

Volume - 2.14 cm<sup>3</sup>  
 Density - 1.33 gm/cm<sup>3</sup>

Volume - .103 cm<sup>3</sup>  
 Density - 1.27 gm/cm<sup>3</sup>

Deflection ( $\theta$ ) in Degrees for a Given Field

$\theta$  - 3/4°  
 Tan  $\theta$  - .013

$\theta$  - 1 1/2°  
 Tan  $\theta$  - .026

 $F_G - F_B = .71$  gms. $F_G - F_B = .03$  gms. $\alpha = 2.02$  $\alpha = .720$  $\frac{\rho_o}{\rho_i} = .752$  $\frac{\rho_o}{\rho_i} = .786$

Table II

Data on Measurements of the Cross-Section of the  
Sound Field at a Distance from the Source  
Equal to 30 cm

Distance from an Arbitrary Point Near the Center of the Beam Measured in cm	Deflection of the Air Vane in Degrees
-9	0
-8	0
-7	0
-6	0
-5	1
-4	2 1/2
-3	6
-2	8
-1	8
0	7 1/2
1	6
2	4
3	2
4	1
5	0
6	0
7	0
8	0

Table III

Data for Calibration of Voltage Amplifier  
and Power Amplifier

---

Frequency of Input Signal Maintained  
at 59 kc

---

Input (Volts)	Output (Volts)
0	.5
.1	46
.2	92
.3	120
.4	155
.5	170
.6	180
.7	190
.8	195
.9	200
1.0	200
1.2	200
1.5	205
2.0	205
2.5	205
3.0	210
5.0	215
7.0	220
9.0	220
11.0	217
13.0	210
15.0	205

Table IV

Calibration Data for Voltage Input Vs. Sonic Output  
for the Ammonium Phosphate Crystal Transducer

Audio oscillator operated for 2 hours and power  
amplifier operated for 15 minutes before  
these observations were made

Frequency maintained at 59 kc cathode current  
about 50 m.a.

Volts Input	Deflection of Air Vane in Degrees
10	0
20	0
30	0
40	0
50	0
60	0
70	• 1/4
80	1/4
90	1/2
100	3/4
120	1
140	1 1/2
160	2
180	3
200	4
220	4 1/2
240	7 1/2
260	8 1/2
265	8 1/2



Table V

Voltage Calibration Data for the High Sensitivity  
Inverse Feedback Voltage Amplifier

Column A = Output of the H.P. audio oscillator in volts

Column B = Output of the attenuator in microvolts

Column C = Output of the amplifier in volts

Run #1				Run #2			
A	B	C		A	B	C	
		DC	AC			DC	AC
0	0	1.05	0	0	0	1.10	0
.1	.316	1.10	.1	.1	.316	1.17	.17
.2	.632	1.24	.28	.2	.632	1.35	.35
.3	.942	1.39	.40	.3	.942	1.55	.54
.4	1.264	1.55	.55	.4	1.264	1.75	.70
.5	1.580	1.75	.71	.5	1.580	1.95	.88
.6	1.896	1.90	.85	.6	1.896	2.17	1.08
.7	2.313	2.10	1.04	.7	2.212	2.37	1.25
.8	2.528	2.31	1.21	.8	2.528	2.60	1.45
.9	2.844	2.48	1.35	.9	2.844	2.82	1.63
1.0	3.160	2.68	1.52	1.0	3.160	3.02	1.82
1.1	3.416	2.83	1.65	1.1	3.416	3.28	2.04
1.2	3.792	3.04	1.82	1.2	3.792	3.49	2.20
1.3	4.102	3.20	1.95	1.3	4.102	3.69	2.37
1.4	4.424	3.41	2.13	1.4	4.424	3.90	2.55
1.5	4.740	3.57	2.27	1.5	4.740	4.10	2.69
1.6	5.056	3.79	2.46	1.6	5.056	4.30	2.85
1.7	5.362	3.95	2.58	1.7	5.362	4.55	3.04
1.8	5.688	4.17	2.74	1.8	5.688	4.80	3.20
1.9	6.004	4.35	2.87	1.9	6.004	5.10	3.40
2.0	6.320	4.60	3.04	2.0	6.320	5.40	3.60
3.0	9.480	--	--	3.0	9.480	7.60	5.40
4.0	12.640	--	--	4.0	12.640	9.70	7.10

Table VI

## Frequency Response of Driver and Transducer

(Gain on H.P. Audio Oscillator, primary source of oscillator, at 36.5 output of amplifier read by means of an RCA Volttohmyst)

Column A = Deflection of air vane in degrees

Column B = Voltage input to transducer

Column C = Cathode current in milliamperes

Frequency (KC)	A	B	C	Frequency (KC)	A	B	C
16	2	80	60	43	0	131	62
17	2	79	60	44	1/2	145	62
18	2	70	60	45	1	180	60
19	2	89	60	46	2	194	60
20	2	121	61	47	3	202	60
21	1	110	62	48	3	215	56
22	1	114	62	49	4 1/2	212	55
23	1	132	60	50	5 1/2	193	55
24	2	159	60	51	5	169	56
25	3	155	58	52	3 1/2	138	56
26	3 1/2	118	59	53	4	131	57
27	3 1/2	124	58	54	5 1/2	134	57
28	3	146	57	55	5 1/2	150	56
29	3	164	56	56	5 1/2	109	55
30	3	186	56	57	6	194	54
31	1 1/2	160	60	58	5	220	51
32	1 1/2	122	62	59	4 1/2	224	47
33	-----	---	--	60	3	218	48
34	0	96	62	61	3	211	52
35	0	90	63	62	2 1/2	195	56
36	0	90	63	63	2	180	60
37	0	90	63	64	1 1/2	160	60
38	0	91	63	65	1	141	61
39	0	95	63	66	1/2	130	61
40	0	102	63	67	1/2	119	62
41	0	110	63	68	1/2	108	62
42	0	120	63	69	0	100	63
				70	0	90	63

## BIBLIOGRAPHY AND REFERENCES

1. Joule, J.P., Phil. Mag. III, 30, 76, 1847.
2. Curie, J. and P., Acad. Sci., Paris, 91, 294, 1880.
3. Raleigh, Lord, Phil. Mag. VI, 10, 364, 1905.
4. Richards, W.T., Proc. Natl. Acad., Wash., 15, 310, 1929.
5. Greutzmacher, J., Z. Phys., 96, 342, 1935.
6. Bergmann, Ultrasonics.
7. Rock, Fox, and Hertzfelder, Phys. Rev. 329, Sept., 1946.
8. Radio News 50, Nov., 1946.
9. King, L.V., Proc. Roy. Soc., London, A, 147, 212, 1934.
10. A Table of Bessel Functions, Brit. Assoc. Rep., p. 221, 1925.
11. Koerber, F., Zeits. f Phys. Chemie, 67, 212, 1909.
12. Gucker and Meldrum, Physical Chemistry.
13. Gucker and Meldrum, Physical Chemistry.
14. Roberts, J.K., Heat and Transmission.
15. Raleigh, Lord, Theory of Sound.